Electronic Supplementary Material (ESI) for Chemical Communications.

Supporting Information

Phosphinosilylenes as a novel ligand system for heterobimetallic complexes

Nora C. Breit,[a] Carsten Eisenhut[a] and Shigeyoshi Inoue*[a,b]

a) Technische Universität Berlin, Anorganische Chemie, Straße des 17. Juni 135, Sekr. C2, D-10623 Berlin, Germany.
b) Technische Universität München, Institute of Silicon Chemistry and Catalysis Research Center, Lichtenbergstraße 4, D-85748 Garching, Germany.

Contents

1. Experimental Part

General Procedures. All experiments and manipulations were carried out under dry oxygen-free atmosphere using standard Schlenk techniques or in an MBraun inert atmosphere dry box containing an atmosphere of purified nitrogen. Solvents were dried using an M Braun purification system and stored over 3 Å molecular sieves. Ethylenebis(triphenylphosphine) platinum(0) (Aldrich) and nonacarbonyl diiron (ABCR, 99%) were used as received. Iron pentacarbonyl (Acros Organics) was condensed and hexacarbonyltungsten (Merck, 98%) was sublimed prior to use. Phosphinosilylene **1** was prepared according to the literature.[1] The deuterated solvents were degassed by freeze-pump-thaw technique and stored over 3 Å molecular sieves. The ^{1}H, $^{13}C\{^{1}H\}$, $^{29}Si\{^{1}H\}$, $^{31}P\{^{1}H\}$, ^{31}P, $^{195}Pt\{^{1}H\}$ spectra were recorded on Bruker Avance II 200 MHz, 400 MHz and Bruker Avance III 500 MHz Spectrometers. ^{1}H chemical shifts were referenced to the residual protons of C_6D_6 at 7.15 ppm. $^{13}C\{^{1}H\}$ chemical shifts were referenced to the carbon atoms of C_6D_6 at 128.00 ppm and 22.50 ppm for the carbons in thf-d_8. The $^{29}Si\{^{1}H\}$ NMR spectra were referenced to tetramethylsilane as an external standard, $^{31}P\{^{1}H\}$ and ^{31}P spectra were externally calibrated with H_3PO_4 in sealed capillaries and the $^{195}Pt\{^{1}H\}$ NMR spectrum was calibrated to $K_2[PtCl_4]$ as an external standard. Melting points were determined from vacuum sealed capillaries on an electronic "Melting point tester" device from BSGT company and are uncorrected. For this purpose samples were sealed off in capillaries under vacuum and heated slowly to observed decomposition or melting. High resolution mass spectra were recorded on an Orbitrap LTQ XL of Thermo Scientific mass spectrometer. Elemental analysis was conducted on a Thermo Finnigan Flash EA 1112 series. IR spectra were recorded on a PerkinElmer Spectrum 100 FTIR.

Single-Crystal X-ray Structure Determinations. Crystals were mounted on a glass capillary in perfluorinated oil and measured in a cold N_2 flow. The data of compounds **2**, **3**, **4**, and **6** were collected on an Oxford Diffraction SuperNova at 150 K (Cu-Kα radiation, λ = 1.5418 Å). The structures were solved by direct methods or Patterson and refined on F2 with the SHELX-97[2] software package. The positions of the hydrogen atoms on carbon were calculated and considered isotropically according to a riding model. All phosphorus hydrides and the platinum hydride were found in the electron density map. The dihedral angles and metal-metal distances of the heterobimetallic complexes **4** and **6** were determined with Mercury 3.7. CCDC 1435730 -1435733 contain the supplementary crystallographic data for this paper. These data can be obtained free of charge via www.ccdc.cam.ac.uk/data_request/cif, or by emailing data_request@ccdc.cam.ac.uk, or by contacting The Cambridge Crystallographic Data Centre, 12, Union Road, Cambridge CB2 1EZ, UK; fax: +44 1223 336033.

Cyclic Voltametry Measurements. The cyclic voltammetry measurements were carried out in a glove box at 295 K with a Biologic SP-150 potentiostat. The three electrode set-up consisted of glassy carbon (disc with 3 mm diameter) as the working electrode, Ag/Ag^{+} as the pseudo reference electrode and a platinum wire as the auxiliary electrode. The iR drop was determined and compensated by using the impedance measurement technique implemented in the EC Lab Software V10.37. The Cp_2Fe/Cp_2Fe^{+} redox couple was used as an internal standard and all cyclic voltammograms are referenced to it. Freshly prepared 1 mM solutions of **3** or **6** in thf (10 mL) with 0.1 M $[nBu_4N][PF_6]$ as supporting electrolyte were used.

Preparation of [LSi{Fe(CO)$_4$}P(TMS)$_2$], 2. Fe(CO)$_5$ (0.27 mL, 2.00 mmol) was added dropwise to a solution of freshly prepared **1** (854 mg, 1.96 mmol) in thf (20 mL) at -40 °C. The reaction mixture was stirred for 16 h at r.t. Volatiles were removed under vacuum. The residue was washed with pentane (4 + 4 + 2 mL) at -30 °C and dried in high vacuum to give analytically pure **2** (929 mg, 78%). Mp. 141-142 °C. ^{1}H NMR (200.13 MHz, C_6D_6, 298 K): δ = 0.54 (d, $^3J_{P\text{-}H}$ = 5.1 Hz, 18 H, TMS), 1.23 (s, 18 H, *t*Bu), 6.8-7.0 (m, 3 H, Ph), 7.37 (m, 1 H, Ph), 7.71 (m, 1 H, Ph) ppm. ^{13}C{^{1}H} NMR (125.76 MHz, C_6D_6, 298 K): δ = 4.4 (d, $^2J_{C\text{-}P}$ = 11.6 Hz, TMS), 31.6 (C*Me$_3$*), 56.3 (*C*Me$_3$), 128.7, 129.4, 130.6, 131.2 (Ph), 168.2 (NCN), 217.2 (CO) ppm. ^{29}Si{^{1}H} NMR (79.49 MHz, C_6D_6, 298 K): δ = 4.5 (d, $^1J_{Si\text{-}P}$ = 18.3 Hz, TMS), 102.6 (d, $^1J_{Si\text{-}P}$ = 116.2 Hz, LSi) ppm. ^{31}P{^{1}H} NMR (MHz, C_6D_6, 298 K): δ = -194.4 (s with satellites: $^1J_{Si\text{-}P}$ = 116.2 Hz and $^1J_{Si\text{-}P}$ = 18.3 Hz). HRMS (APCI, toluene): calcd for $C_{25}H_{42}FeN_2O_4PSi_3^+$, MH$^+$, 605.1534; found, 605.1498, calcd for M$^+$, 604.1461; found, 604.1442. IR (KBr): ν = 2022 (s, CO), 1941 (s, CO), 1904 (s, CO) cm^{-1}. Elemental analysis calcd for $C_{25}H_{41}FeN_2O_4PSi_3$: C 49.66, H 6.83, N 4.63; found C 49.94, H 6.94, N 4.55.

Preparation of [LSi{Fe(CO)$_4$}PH$_2$], 3. A solution of H_2O in thf (1.53 mL, 1.53 mmol) was added dropwise to a solution of **2** (929 mg, 1.53 mmol) in thf (10 mL) at r.t. After being stirred for 2 days, volatiles were removed under vacuum to yield pure **3** (685 mg, 97%). Single crystals suitable for X-ray crystallography can be obtained from diethylether at -28 °C in 69% yield. Mp. 163-164 °C. ^{1}H NMR (500.13 MHz, C_6D_6, 298 K): δ = 1.03 (s, 18 H, *t*Bu), 2.50 (d, $^1J_{P\text{-}H}$ = 188 Hz, 2 H, PH$_2$), 6.65 (m, 1 H, Ph), 6.78 (m, 2 H, Ph), 6.89 (m, 1 H, Ph) ppm. ^{13}C{^{1}H} NMR (125.76 MHz, C_6D_6, 298 K): δ = 31.3 (C*Me$_3$*), 55.7 (*C*Me$_3$), 128.4 (Ph), 129.0 (Ph), 130.5 (Ph), 130.7 (Ph), 169.2 (NCN), 216.1 (CO) ppm. ^{29}Si{^{1}H} NMR (99.36 MHz, C_6D_6, 298 K): δ = 112.8 (d, $^1J_{Si\text{-}P}$ = 62 Hz) ppm. ^{31}P{^{1}H} NMR (81.01 MHz, C_6D_6, 298 K): δ = -198.5 (s with satellites) ppm. ^{31}P NMR (202.46 MHz, C_6D_6, 298 K): δ = -198.6 (*t*, $^1J_{P\text{-}H}$ = 188 Hz) ppm. HRMS (APCI, toluene): calcd for $C_{19}H_{26}FeN_2O_4PSi^+$ as M$^+$, 461.0743; found, 461.0739. IR (KBr): ν = 2025 (s, CO), 1946 (s, CO), 1913 (s, CO) cm^{-1}. Elemental analysis calcd for $C_{19}H_{26}FeN_2O_4PSi$: C 49.47, H 5.68, N 6.07; found C 49.55, H 5.52, N 6.13.

Preparation of [LSi{Fe(CO)$_4$}PH$_2${W(CO)$_5$}], 4. A solution of W(CO)$_6$ (83 mg, 0.24) in thf (4mL) was treated for 2h with UV light (320-400 nm, 500 W). The in situ formed W(CO)$_5$·thf solution is then added to a solution of **3** (83 mg, 0.18 mmol) at r.t. After being stirred for 2 hours, volatiles were removed under vacuum. The product was extracted with pentane (8.0 mL) and the amount of solvent is reduced under vacuum. The solid obtained at -28 °C is washed at low temperature with pentane (1 mL). After drying under vacuum, as much W(CO)$_6$ as possible was removed by sublimation. However, the resulting solid (85 mg, would have been 60%, if pure) still contained some tungsten carbonyl containing impurities as observed by ^{13}C NMR spectroscopy. ^{1}H NMR (200.13 MHz, C_6D_6, 298 K): δ = 1.02 (s, 18 H, *t*Bu), 3.98 (d, $^1J_{P\text{-}H}$ = 302 Hz, 2 H, PH$_2$), 6.7-7.0 (m, 3 H, ArH), 7.22 (m, 1 H, ArH), 7.36 (m, 1 H, ArH) ppm. ^{13}C{^{1}H} NMR (125.75 MHz, C_6D_6, 298 K): δ = 31.0 (C*Me$_3$*), 56.2 (*C*Me$_3$), 128.4, 128.6, 129.8, 131.2 (Ar*C*), 172.1 (N*C*N), 196.4 (d, $^2J_{C\text{-}P}$ = 5.6 Hz, W{CO}$_5$), 215.1 (Fe{CO}$_4$) ppm. ^{29}Si{^{1}H} NMR-DEPT (39.76 MHz, C_6D_6, 298 K): δ = 98.0 (d, $^1J_{Si\text{-}P}$ = 23.8 Hz). ^{31}P{^{1}H} NMR (81.01 MHz, C_6D_6, 298 K): δ = -165.2 (s with satellites, $^1J_{P\text{-}W}$ = 187 Hz, $^1J_{Si\text{-}P}$ = 23.8 Hz) ppm. ^{31}P NMR (81.01 MHz, C_6D_6, 298 K): δ = -165.2 (t, $^1J_{P\text{-}H}$ = 302 Hz, with satellites, $^1J_{P\text{-}W}$ = 187 Hz). HRMS (APCI, toluene): Calcd for $C_{24}H_{26}FeN_2O_9PSiW$, [M+H]$^+$, 784.9998 ; found, 785.0005. IR (KBr): ν_{CO} = 2074 (sharp), 2040 (strong), 2010-1830 (very broad area), 1989 (shoulder), 1903 (strong) cm^{-1}.

Preparation of [LSi{Fe(CO)$_4$}PH$_2${Fe(CO)$_4$}], 5. Thf (10 mL) was added to a flask with **3** (98 mg, 0.21 mmol) and Fe$_2$(CO)$_9$ (80 mg, 0.22 mmol) at -50 °C. The reaction mixture was allowed to get to room temperature as the cold bath did as it was stirred for 16 h. Volatiles were removed under vacuum. The product was extracted with hexane (8 mL) and the resulting solution was concentrated to approximately 1 mL. At -28 °C **5** was obtained as a beige colored solid (70 mg, 52%). Mp. 111 °C.^{1}H NMR (400.13 MHz, C_6D_6, 298 K): δ = 1.02 (s, 18 H, *t*Bu), 3.90 (d, $^1J_{P\text{-}H}$ = 321 Hz, 2 H, PH_2), 6.7-6.9 (m, 3 H, ArH), 7.3-7.4 (m, 2 H, Ar-H) ppm. $^{13}C\{^1H\}$ NMR (100.61 MHz, C_6D_6, 298 K): δ = 30.8 (C*Me*$_3$), 56.3 (*C*Me$_3$), 129.9, 131.2 (Ar-C), 173.3 (N*C*N), 214.4 (d, $^2J_{P\text{-}C}$ = 17 Hz, P->Fe(CO)$_4$), 214.9 (Si->Fe(CO)$_4$) ppm. ^{31}P NMR (161.98 MHz, C_6D_6, 298 K): δ = -102.3 (t, $^1J_{P\text{-}H}$ = 321 Hz) ppm. $^{31}P\{^1H\}$ NMR (81.01 MHz, C_6D_6, 298 K): δ = -102.3 (s with satellites $^1J_{Si\text{-}P}$ = 25 Hz) ppm. $^{29}Si\{^1H\}$ NMR (79.49 MHz, C_6D_6, 298 K): δ = 99.2 (d, $^1J_{Si\text{-}P}$ = 25 Hz) ppm. IR (KBr): ν_{CO} = 2055 (sharp), 2035 (sharp), 1983 (weak shoulder), 1970 (shoulder), 1955 (broad, strong), 1938 (broad, strong), 1924 (weak shoulder), 1907 (broad, strong) cm^{-1}. HRMS (APCI, toluene): calcd for $C_{23}H_{26}Fe_2N_2O_8PSi^+$(M$^+$), 628.9889; found, 628.9897. EA calcd for $C_{23}H_{26}Fe_2N_2O_8PSi$: C, 43.90; H, 4.17; N, 4.45; found: C, 44.52; H, 4.11; N, 4.31.

Preparation of [LSi{Fe(CO)$_4$}PH{PtH(PPh$_3$)$_2$}], 6. Toluene (15 mL) was added to LSi{Fe(CO)$_4$}PH$_2$, **3** (152 mg, 0.33 mmol) and $(C_2H_4)Pt(PPh_3)_2$ (248 mg, 0.33 mmol) at -30 °C and the reaction mixture is stirred for 1 h at low temperature. When precipitation is observed and completed, the over standing solution is removed and the solid is washed with toluene (2 x 4 mL) at -50 °C. The dried solid (316 mg) is dissolved in thf (2 mL) and crystalline **6** (233 mg, 60%) is obtained at -28 °C. Mp. 146 °C (decomposition). ^{1}H NMR (400.13 MHz, C_6D_6, 298 K): -4.47 (ddd, $^2J_{P1\text{-}H2}$ = 28 Hz, $^2J_{P3\text{-}H2}$ = 176 Hz, $^2J_{H1\text{-}H2}$ = 21 Hz with platinum satellites $^1J_{H2\text{-}Pt}$ = 906 Hz, 1 H, PtH), 1.35 (s, 18 H, *t*Bu), 2.07 (ddd, $^1J_{P1\text{-}H1}$ = 214 Hz, $^2J_{H1\text{-}H2}$ = 19 Hz with platinum satellites, $^2J_{H2\text{-}Pt}$ = 56 Hz, 1 H, PH), 6.7-6.8 (m, 2 H, Ph of L), 6.80-6.87 (m, 1 H, Ph of L), 6.87-6.95 (m, 18 H, PPh$_3$), 7.48-7.58 (m, 12 H, PPh$_3$), 7.60 (m, 1 H, Ph of L) ppm. $^{13}C\{^1H\}$ NMR (100.61 MHz, thf-d$_8$, 298 K): δ = 29.3 (C*Me*$_3$), 53.0 (*C*Me$_3$), 125.7, 125.8, 125.9, 126.0, 127.8, 127.9, 132.1, 132.3, 132.5, 132.7 (s or m, PPh$_3$), 165.1 (NCN), 215.6 (CO) ppm. $^{29}Si\{^1H\}$ NMR (79.49 MHz, thf-d$_8$, 298 K): δ = 114.8 (m) ppm. ^{31}P NMR (200.46 MHz, thf-d$_8$, 298 K): δ = -105.6 (dddd, $^1J_{P1\text{-}H1}$ = 214 Hz, $^2J_{P1\text{-}H2}$ = 28 Hz, $^2J_{P1\text{-}P2}$ = 139 Hz, $^2J_{P1\text{-}P3}$ = 11 Hz with platinum satellites $^1J_{Pt\text{-}P1}$ = 712 Hz, PH, P1), 20.4 (d, broad $^2J_{P1\text{-}P2}$ = 139 Hz with platinum satellites $^1J_{P2\text{-}Pt}$ = 2536 Hz, PPh$_3$, P2), 25.0 (d, broad $^2J_{P3\text{-}H2}$ = 176 Hz with platinum satellites $^1J_{P3\text{-}Pt}$ = 2081 Hz, PPh$_3$, P3) ppm. $^{31}P\{^1H\}$ NMR (161.98 MHz, thf-d8, 298 K): δ = -105.6 (dd, $^2J_{P1\text{-}P2}$ = 139 Hz, $^2J_{P1\text{-}P3}$ = 11 Hz with platinum satellites $^1J_{Pt\text{-}P1}$ = 712 Hz, PH, P1), 19.3 (dd, $^2J_{P2\text{-}P3}$ = 15 Hz, $^2J_{P2\text{-}P1}$ = 138 Hz with platinum satellites $^1J_{Pt\text{-}P2}$ = 2542 Hz, P2), 25.1 (dd in shape of a psdt ^{2}J= 11 Hz, ^{2}J = 15 Hz with platinum satellites $^1J_{Pt\text{-}P3}$ = 2082 Hz, P3) ppm. $^{195}Pt\{^1H\}$ NMR (86.01 MHz, thf-d$_8$, 298 K): δ = -5035.5 (ddd, $^1J_{Pt\text{-}P1}$ = 713 Hz, $^1J_{Pt\text{-}P2}$ = 2540 Hz, $^1J_{Pt\text{-}P3}$ = 2090 Hz) ppm. HRMS (ESI, thf): calcd for $C_{55}H_{56}FeN_2O_4P_3PtSi^+$, MH$^+$, 1179.2193 (), 1180.2214 () and 1181.2215 (); found, 1179.2200 (), 1180.2229 () and 1181.2244 (). IR (KBr): ν_{CO} = 2014 (s, CO), 1933 (s, CO), 1890 (s, CO). EA calcd for $C_{55}H_{55}FeN_2O_4P_3PtSi$: C 55.94, H 4.78, N 2.37; found: C 55.92, H 4.51, N 2.04.

The ^{1}H and ^{13}C NMR signals of the Ph group in the amidinato ligand could not be assigned due to the overlap with the more intense signals of the PPh$_3$ groups.

2. NMR Spectra of Compounds 2-6.

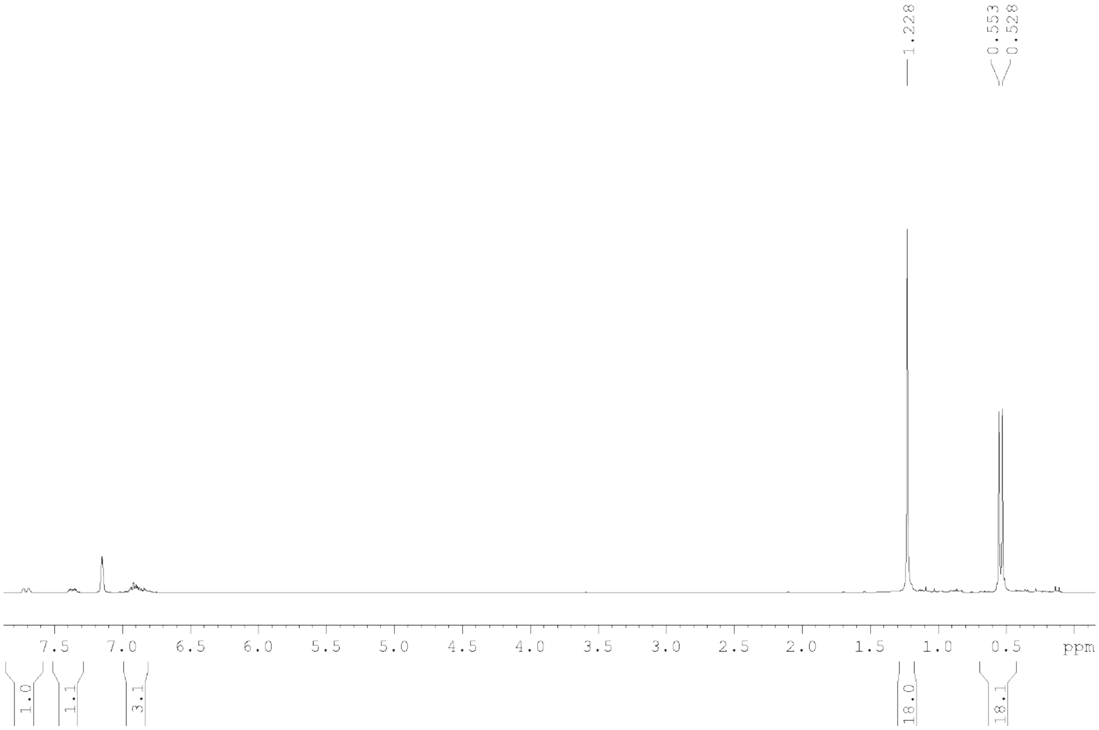

Figure S1. ^{1}H NMR spectrum of compound [LSi{Fe(CO)$_4$}P(TMS)$_2$], **2**.

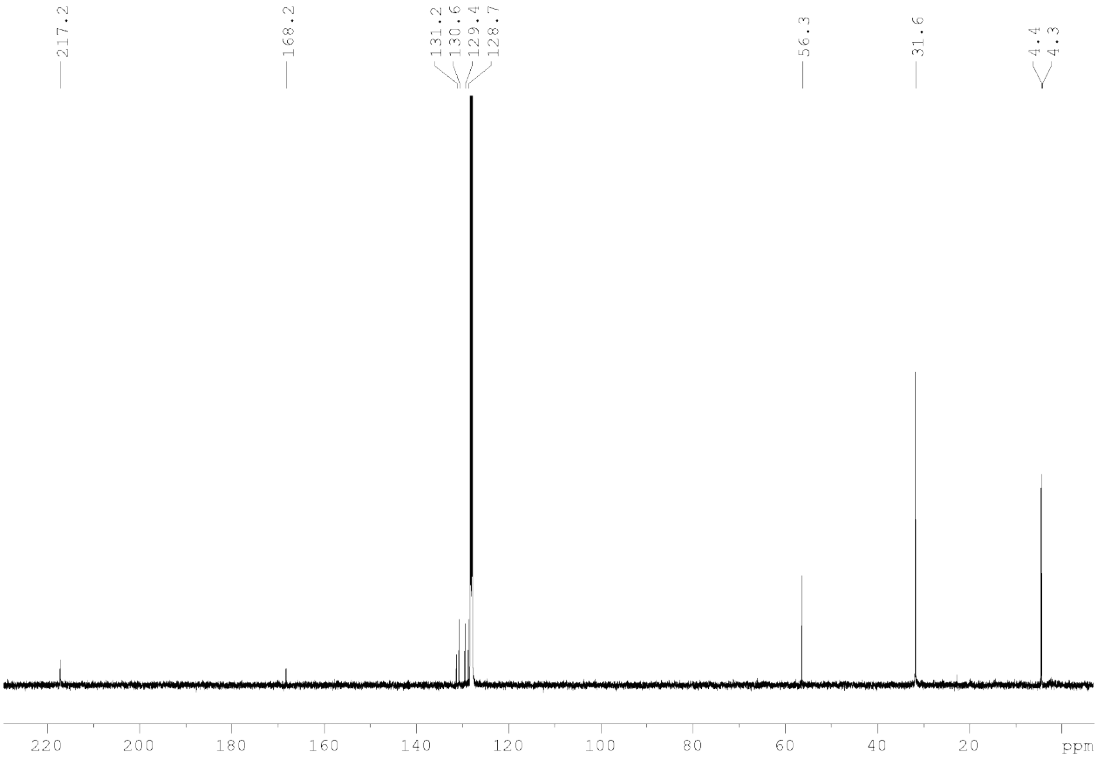

Figure S2. ^{13}C{^{1}H} NMR spectrum of compound [LSi{Fe(CO)$_4$}P(TMS)$_2$], **2**.

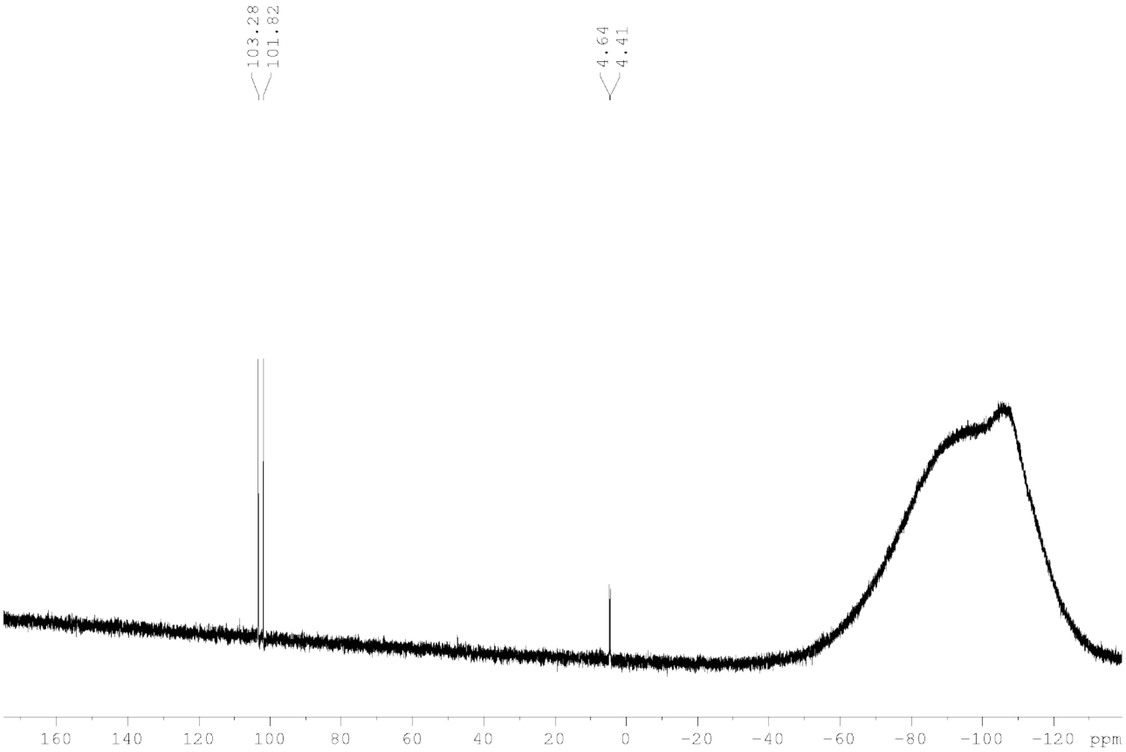

Figure S3. $^{29}Si\{^1H\}$ NMR spectrum for compound [LSi{Fe(CO)$_4$}P(TMS)$_2$], **2**.

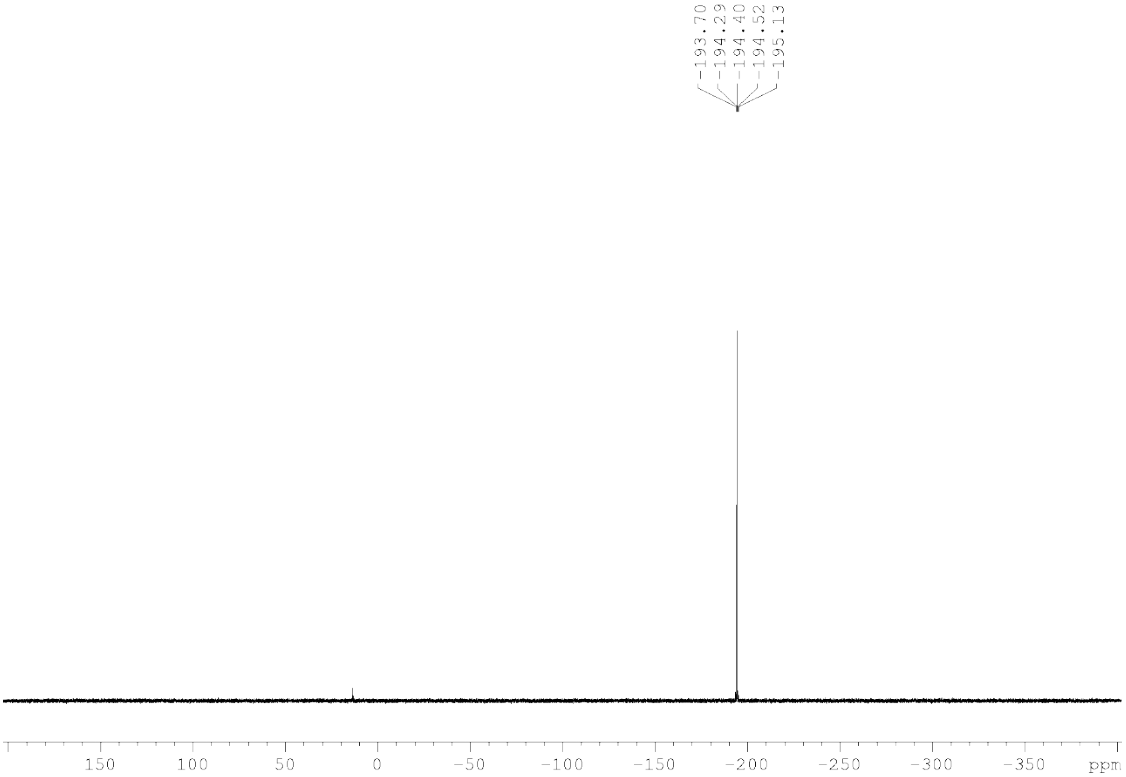

Figure S4. $^{31}P\{^1H\}$ NMR spectrum for compound [LSi{Fe(CO)$_4$}P(TMS)$_2$], **2**.

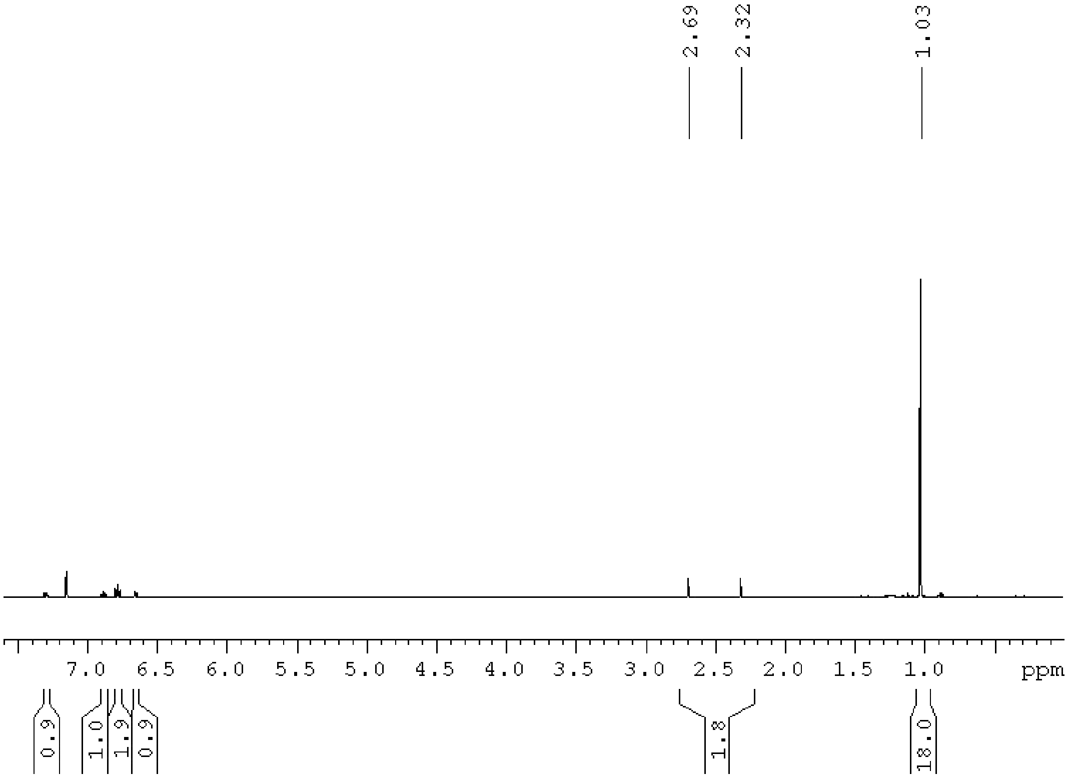

Figure S5. ^{1}H NMR spectrum of compound [LSi{Fe(CO)$_4$}PH$_2$], **3**.

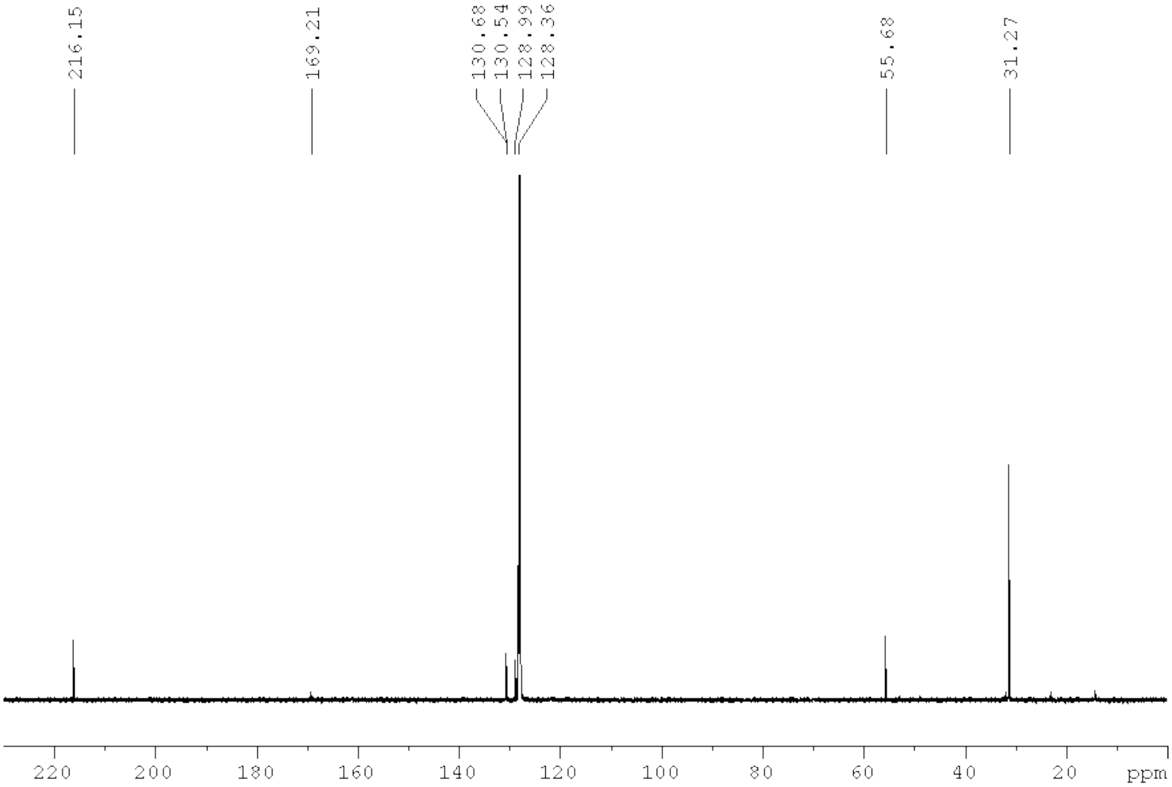

Figure S6. ^{13}C{^{1}H} NMR spectrum of compound [LSi{Fe(CO)$_4$}PH$_2$], **3**.

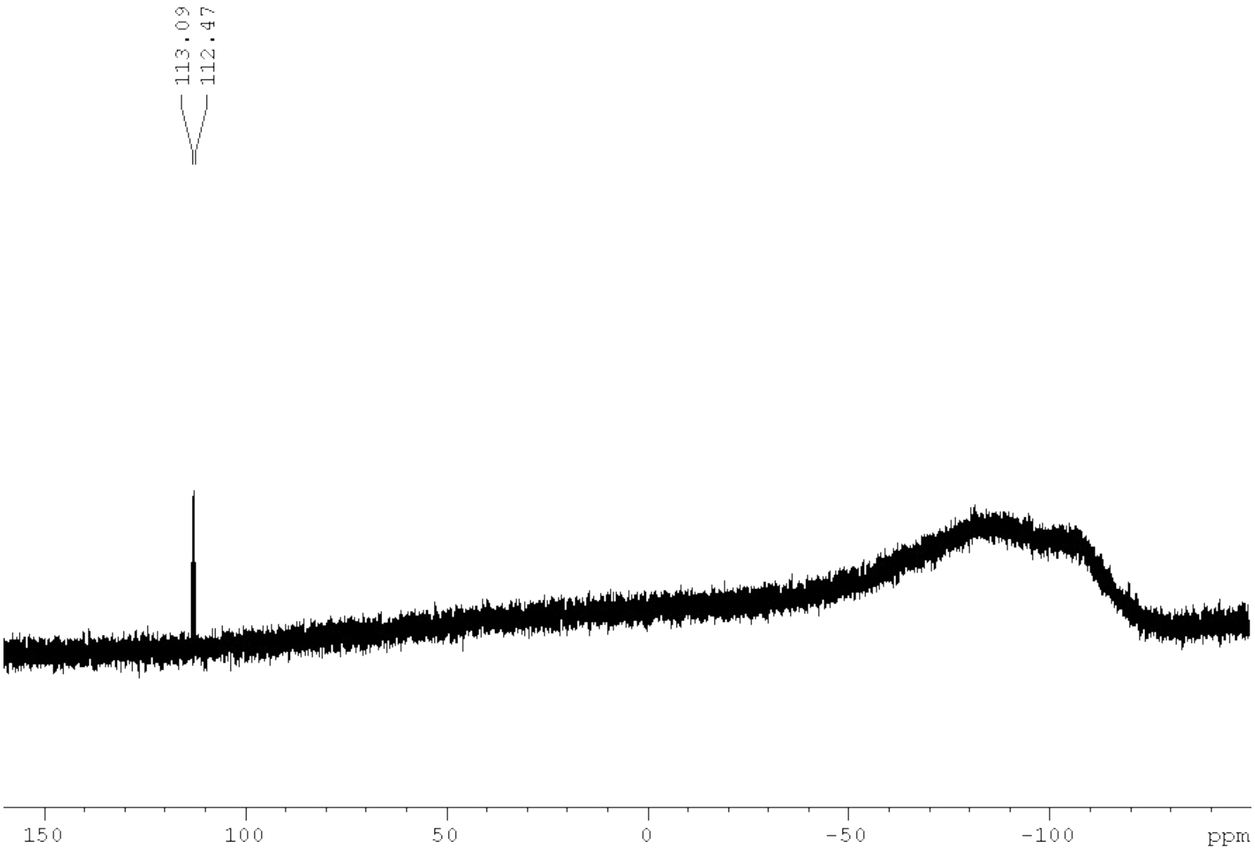

Figure S7. $^{29}Si\{^1H\}$ NMR spectrum of compound $[LSi\{Fe(CO)_4\}PH_2]$, **3**.

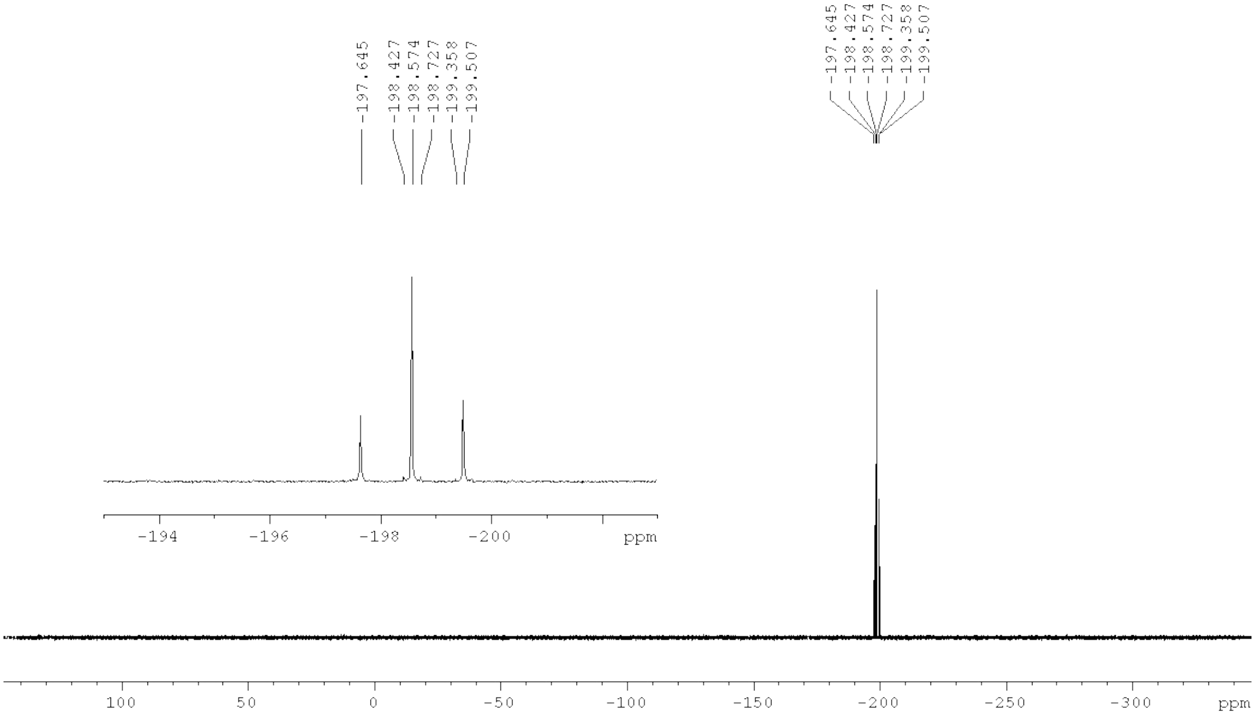

Figure S8. ^{31}P NMR spectrum of compound $[LSi\{Fe(CO)_4\}PH_2]$, **3**.

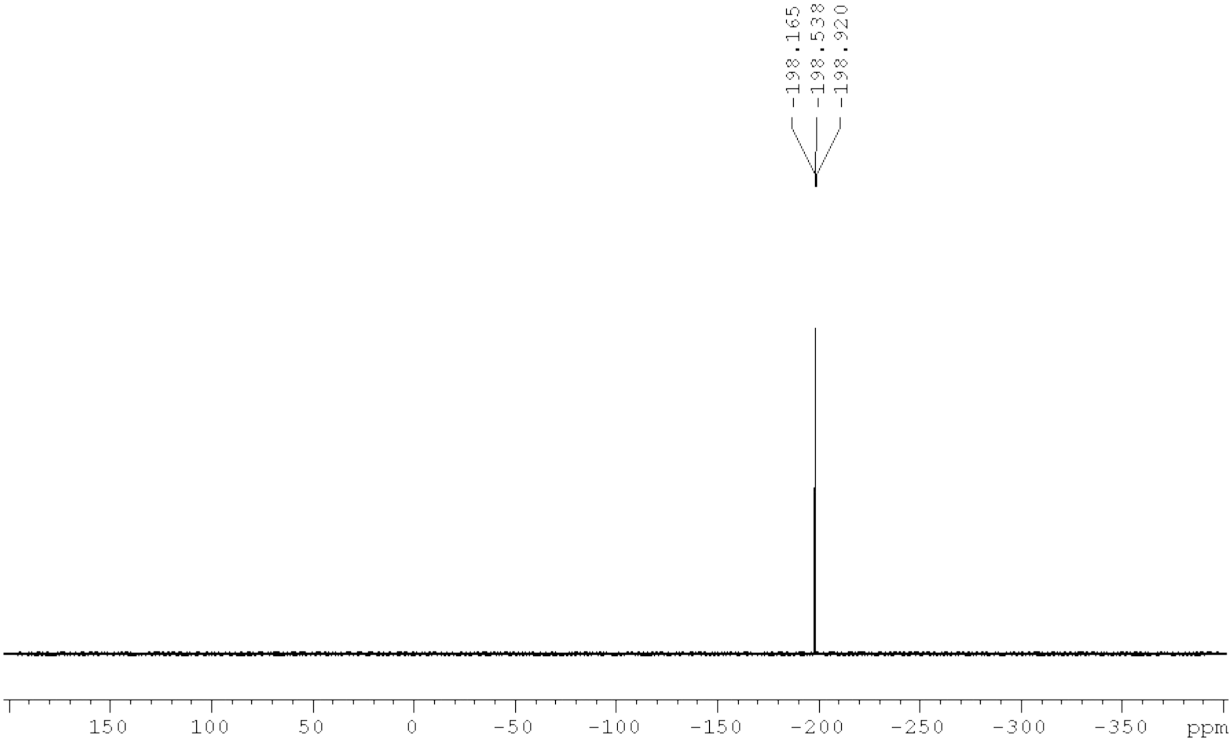

Figure S9. $^{31}P\{^1H\}$ NMR spectrum of compound [LSi{Fe(CO)$_4$}PH$_2$], **3**.

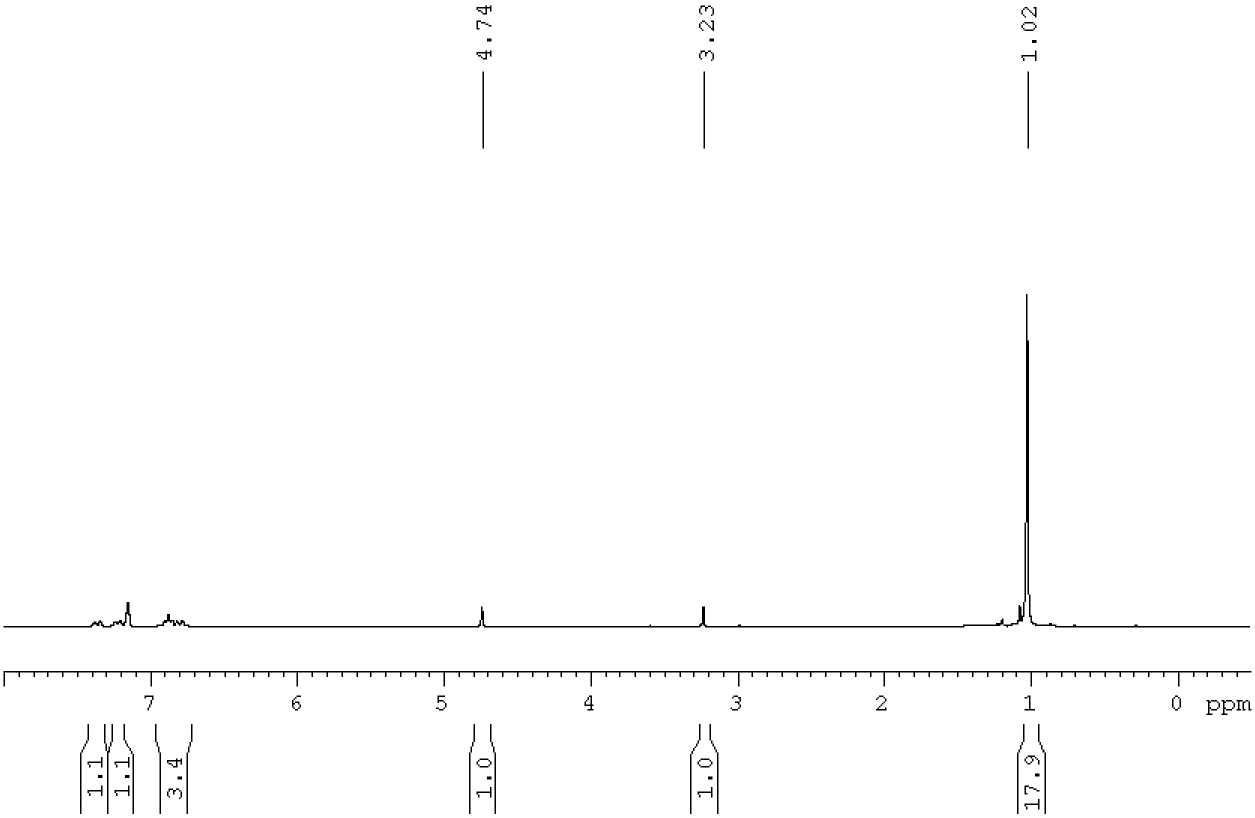

Figure S10. ^1H NMR spectrum of compound [LSi{Fe(CO)$_4$}PH$_2${W(CO)$_5$}], **4**.

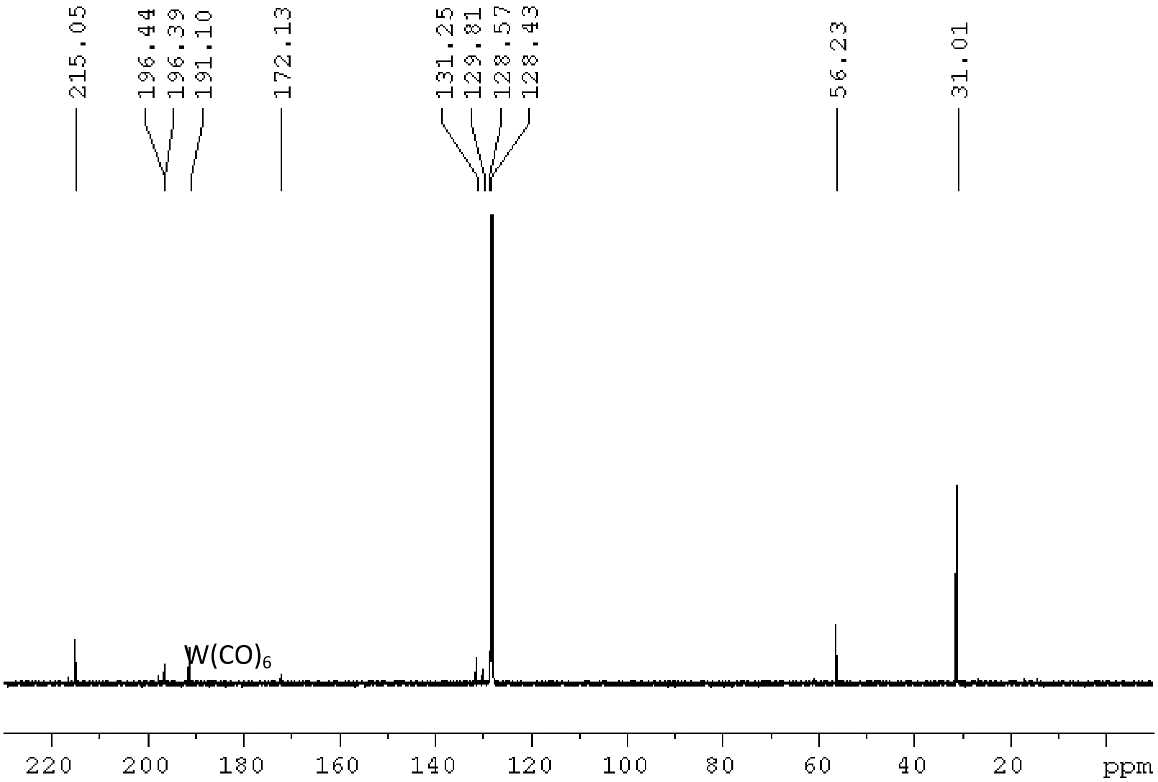

Figure S11. $^{13}C\{^1H\}$ NMR spectrum of compound [LSi{Fe(CO)$_4$}PH$_2${W(CO)$_5$}], **4** in the presence of W(CO)$_6$.

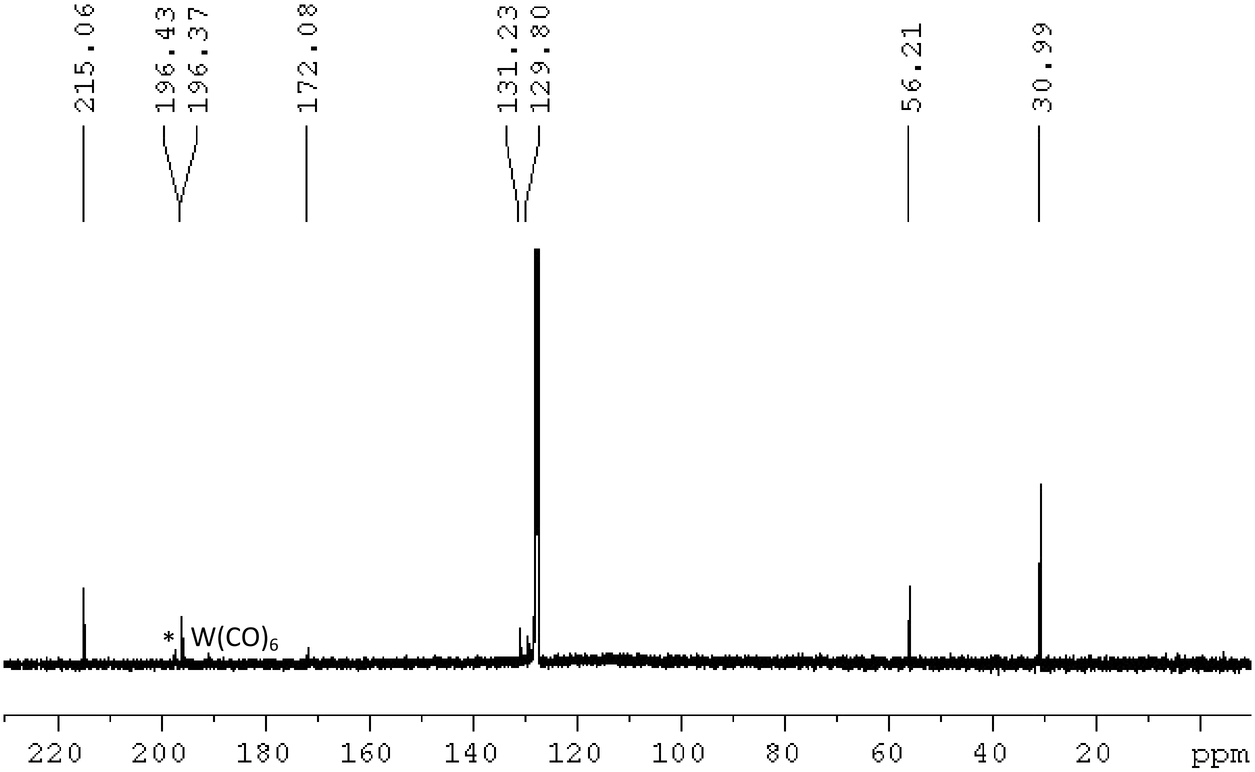

Figure S11. $^{13}C\{^1H\}$ NMR spectrum of compound [LSi{Fe(CO)$_4$}PH$_2${W(CO)$_5$}], **4** in the presence of W(CO)$_6$ and another W(CO)x containing impurity marked with an asterisk.

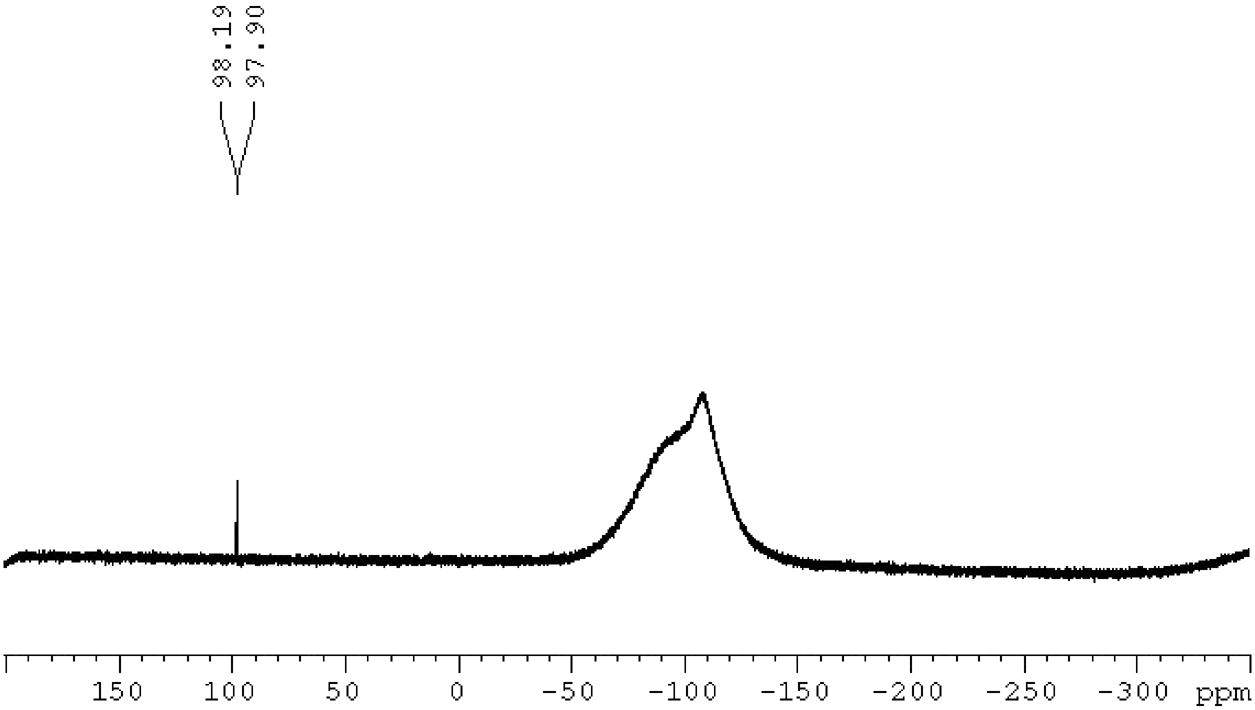

Figure S12. $^{29}Si\{^1H\}$ NMR spectrum of compound [LSi{Fe(CO)$_4$}PH$_2${W(CO)$_5$}], **4**.

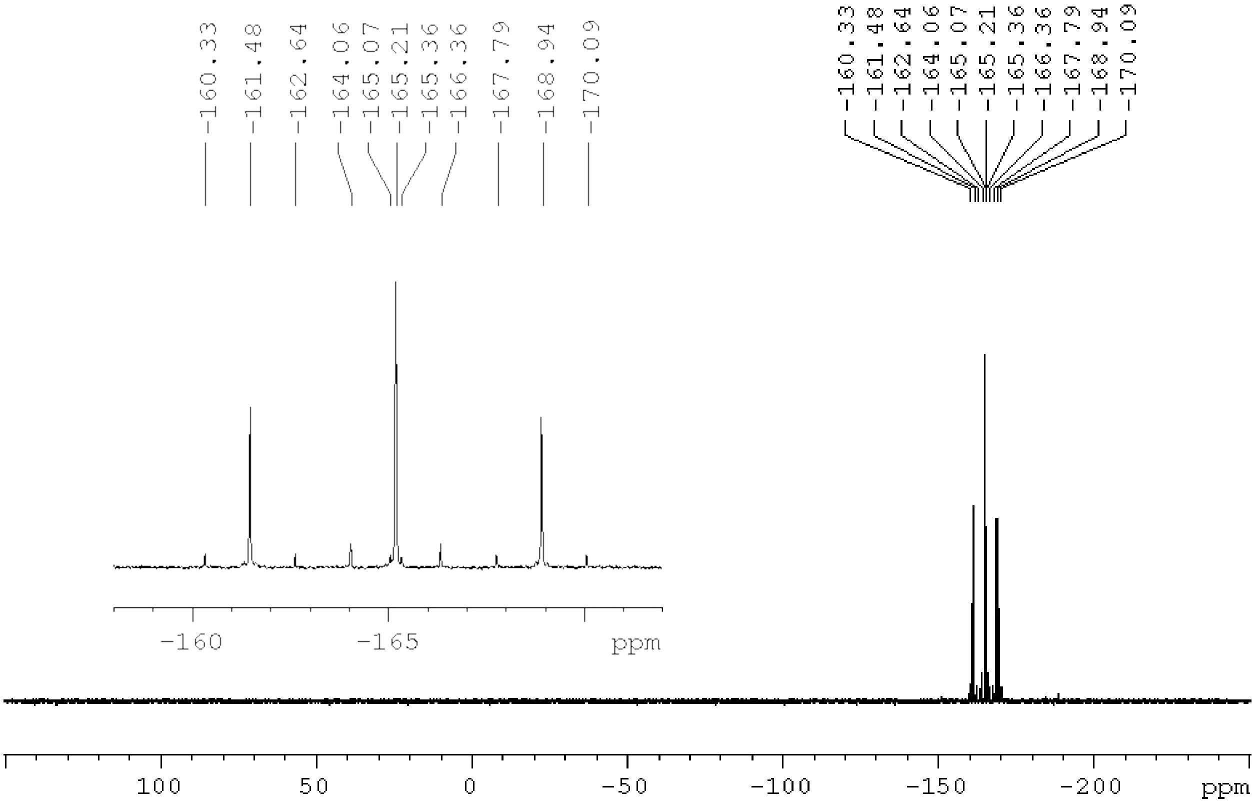

Figure S13. ^{31}P NMR spectrum of compound [LSi{Fe(CO)$_4$}PH$_2${W(CO)$_5$}], **4**.

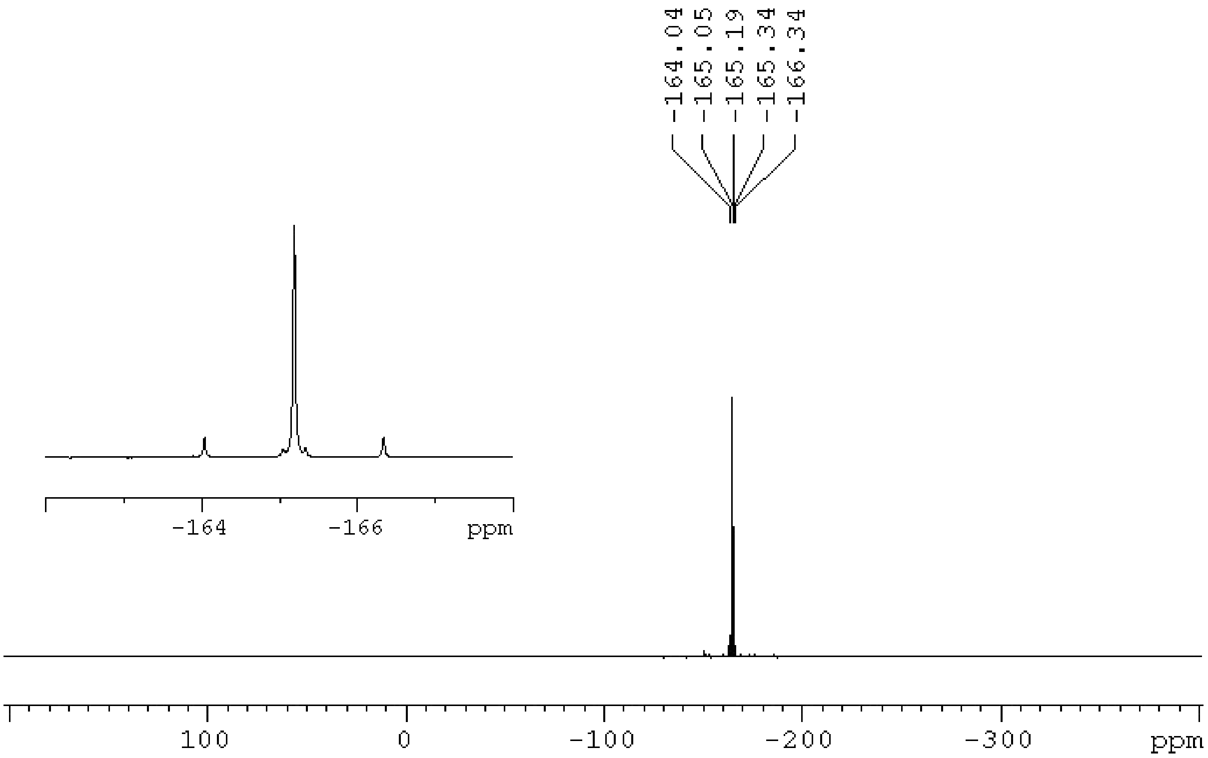

Figure S14. $^{31}P\{^{1}H\}$ NMR spectrum of compound [LSi{Fe(CO)$_4$}PH$_2${W(CO)$_5$}], **4**.

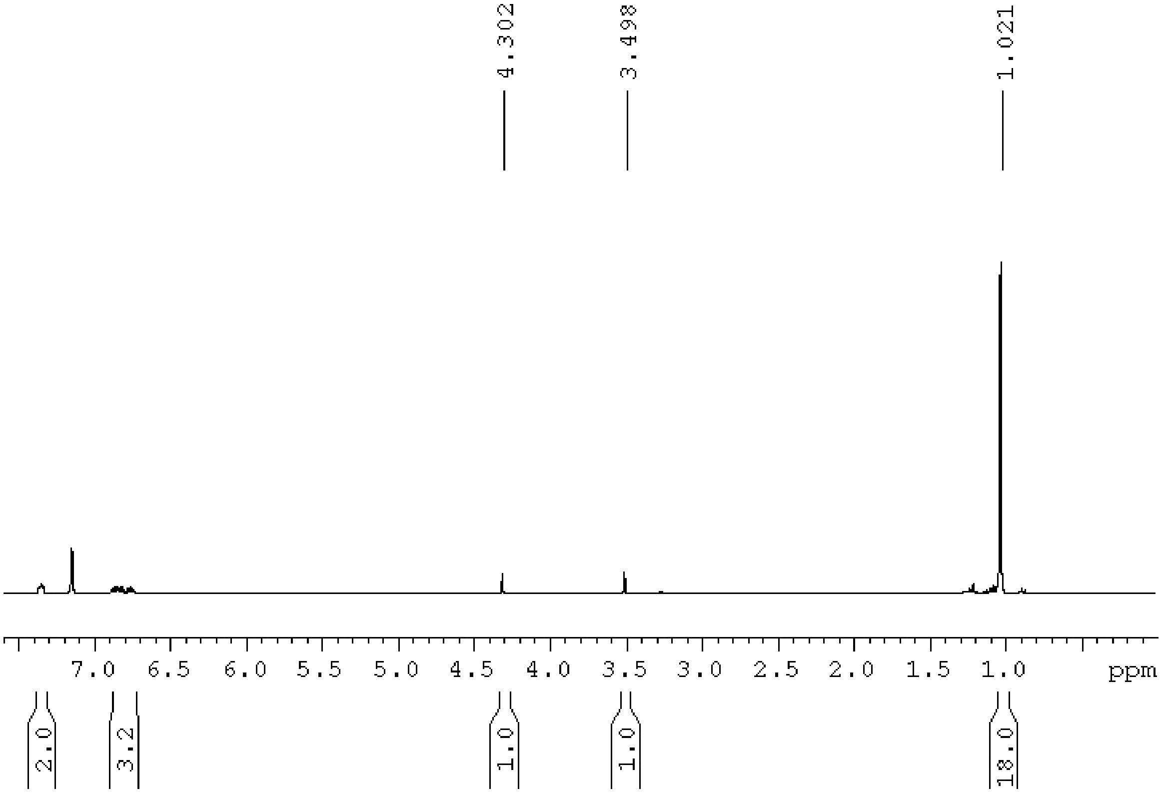

Figure S15. ^{1}H NMR spectrum of compound [LSi{Fe(CO)$_4$}PH$_2${Fe(CO)$_4$}], **5** with little solvent residues (hexane and Et$_2$O).

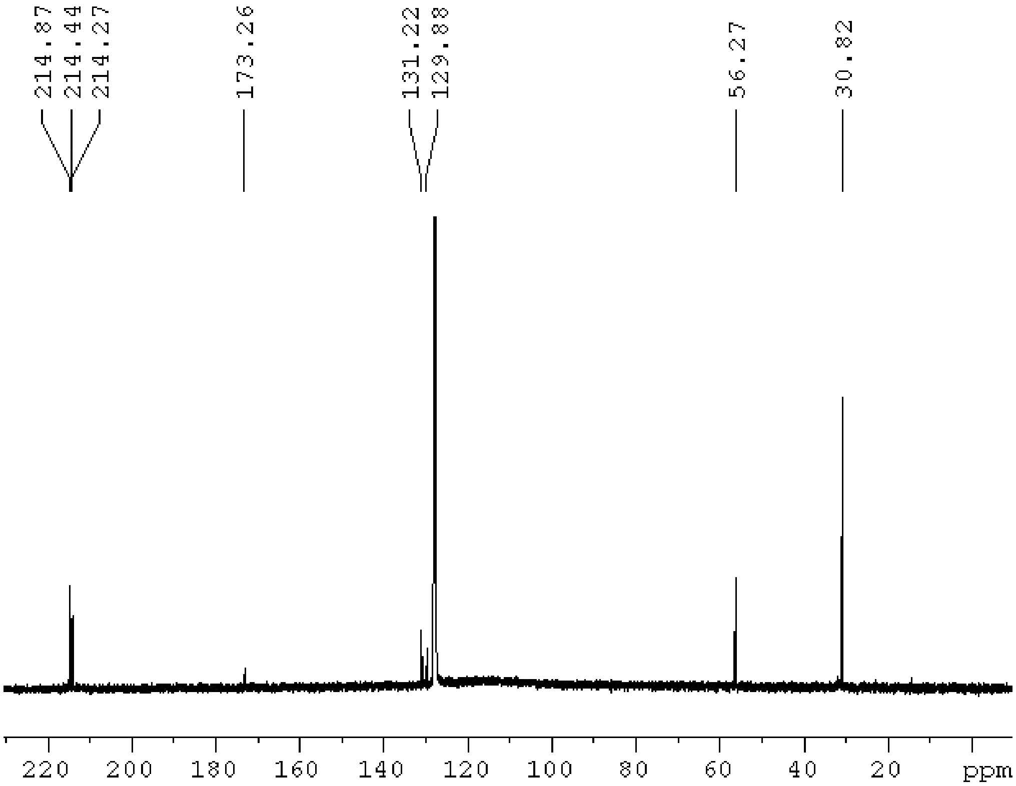

Figure S16. $^{13}C\{^1H\}$ NMR spectrum of compound [LSi{Fe(CO)$_4$}PH$_2${Fe(CO)$_4$}], **5**.

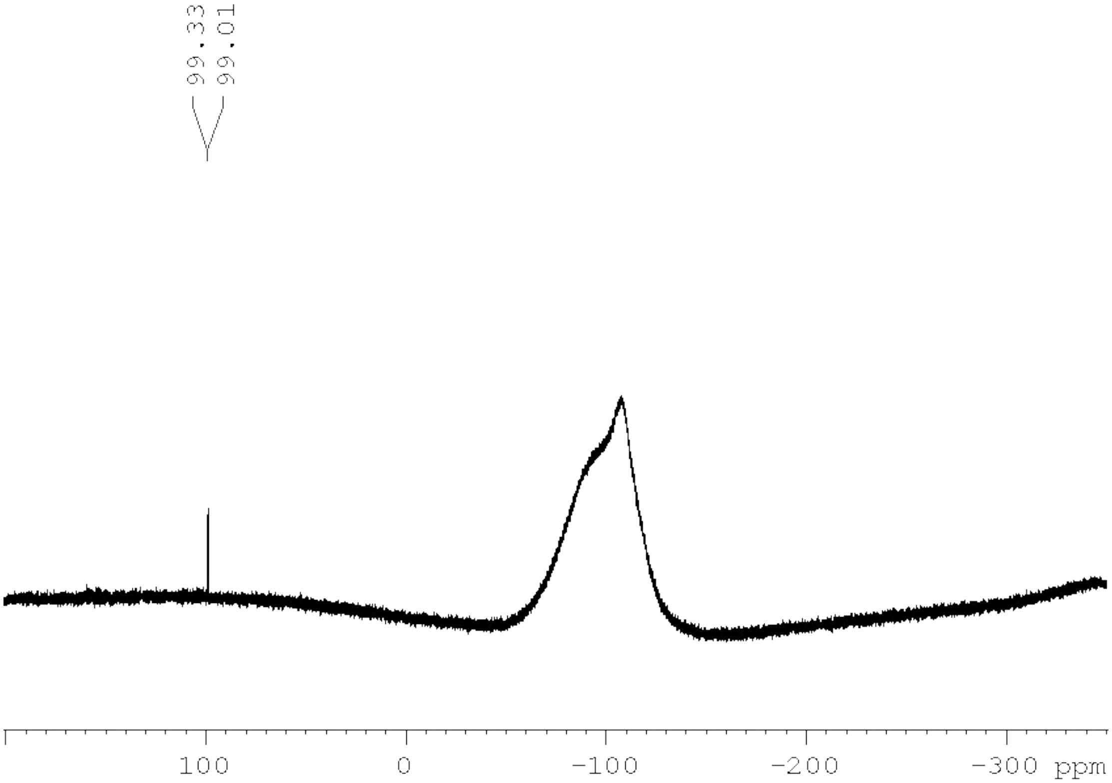

Figure S17. $^{29}Si\{^1H\}$ NMR spectrum of compound [LSi{Fe(CO)$_4$}PH$_2${Fe(CO)$_4$}], **5**.

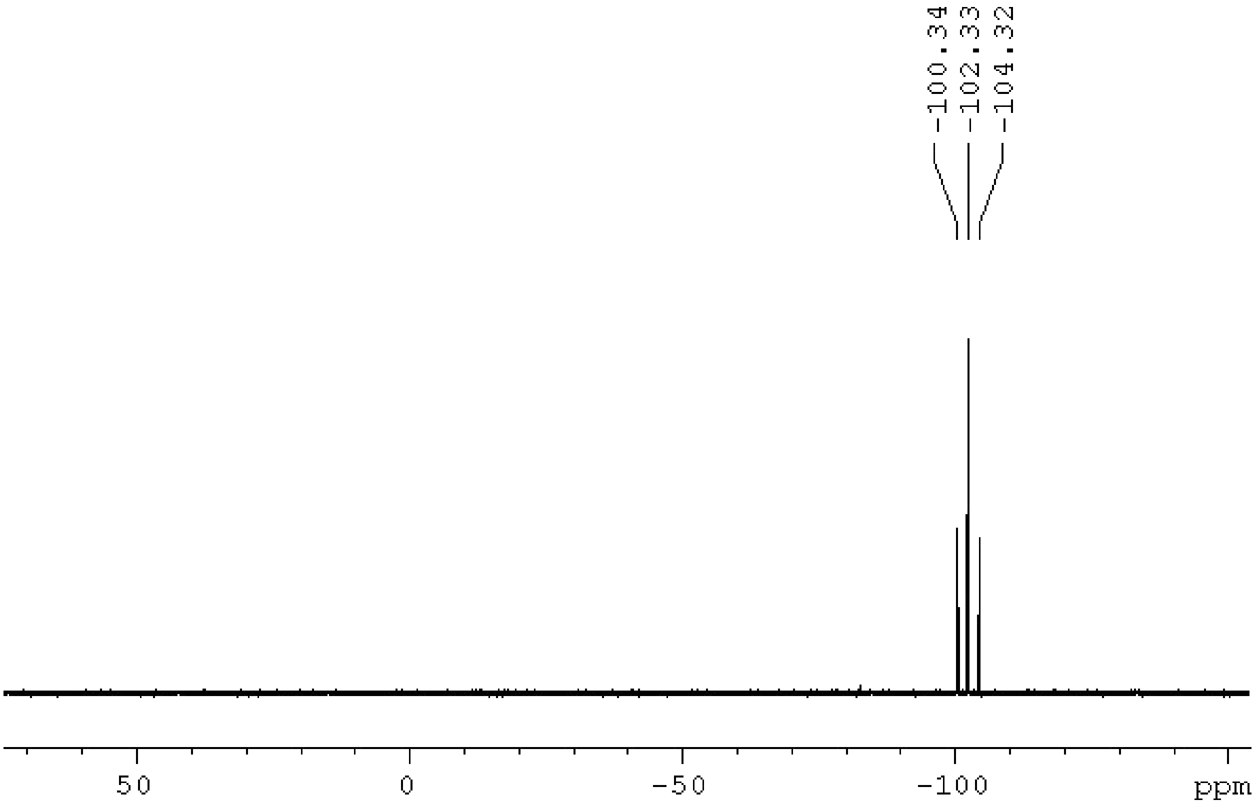

Figure S18. $^{31}P\{^{1}H\}$ NMR spectrum of compound [LSi{Fe(CO)$_4$}PH$_2${Fe(CO)$_4$}], **5**.

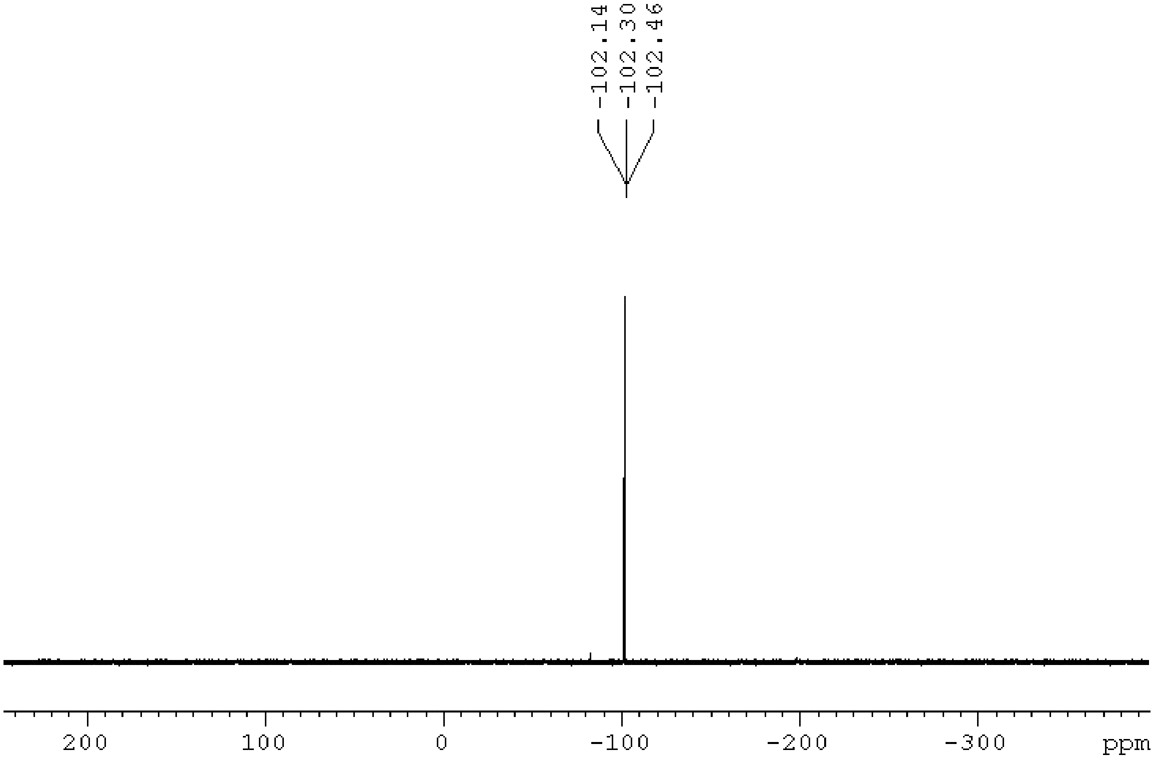

Figure S19. $^{31}P\{^{1}H\}$ NMR spectrum of compound [LSi{Fe(CO)$_4$}PH$_2${Fe(CO)$_4$}], **5**.

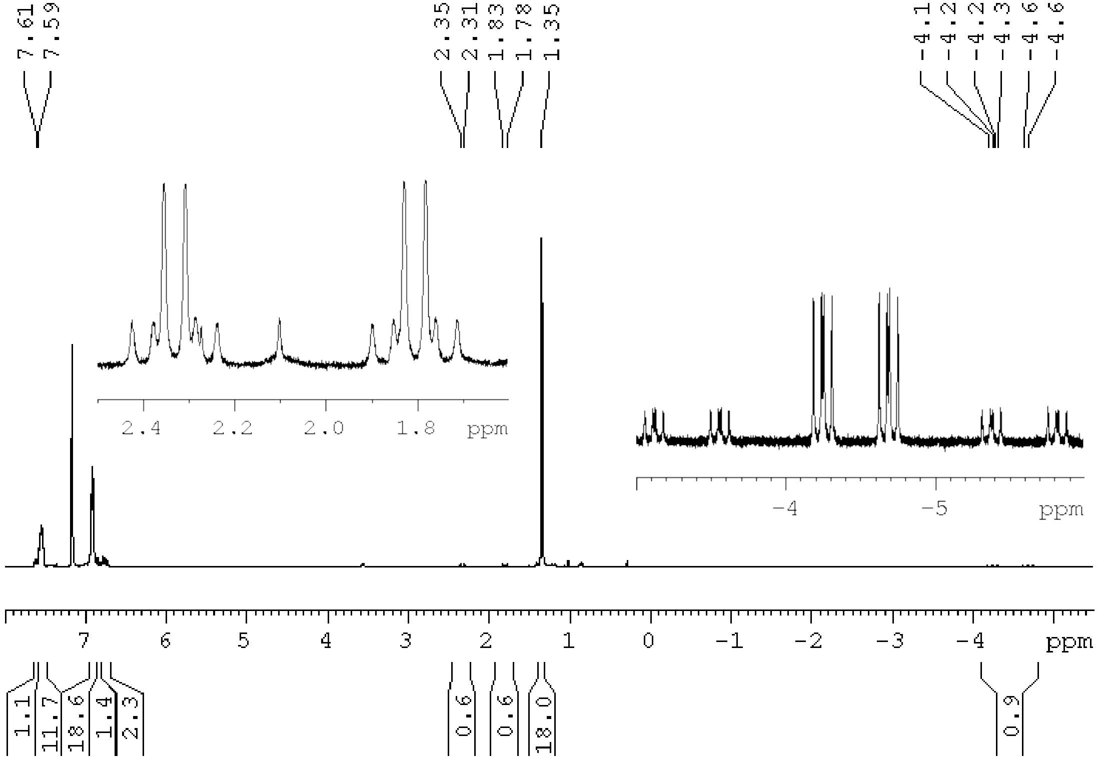

Figure S20. ^{1}H NMR spectrum of compound [LSi{Fe(CO)$_4$}PH{PtH(PPh$_3$)$_2$}], **6**.

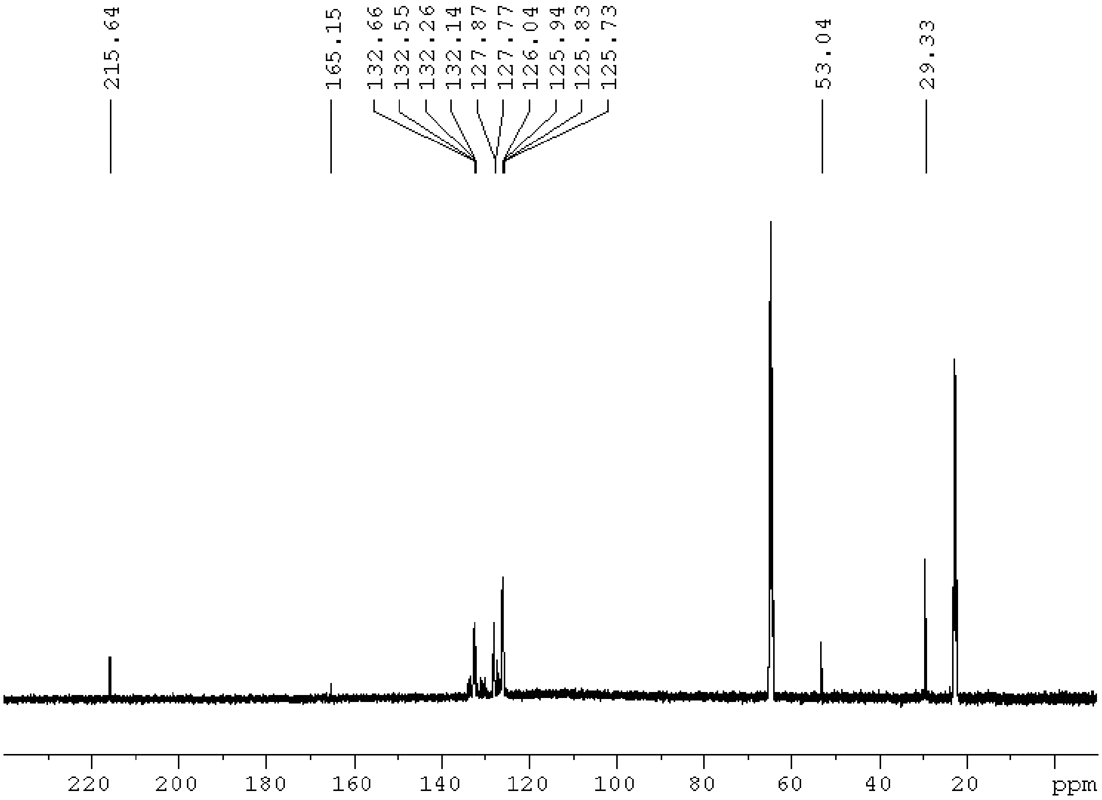

Figure S21. ^{13}C{^{1}H} NMR spectrum of compound [LSi{Fe(CO)$_4$}PH{PtH(PPh$_3$)$_2$}], **6**.

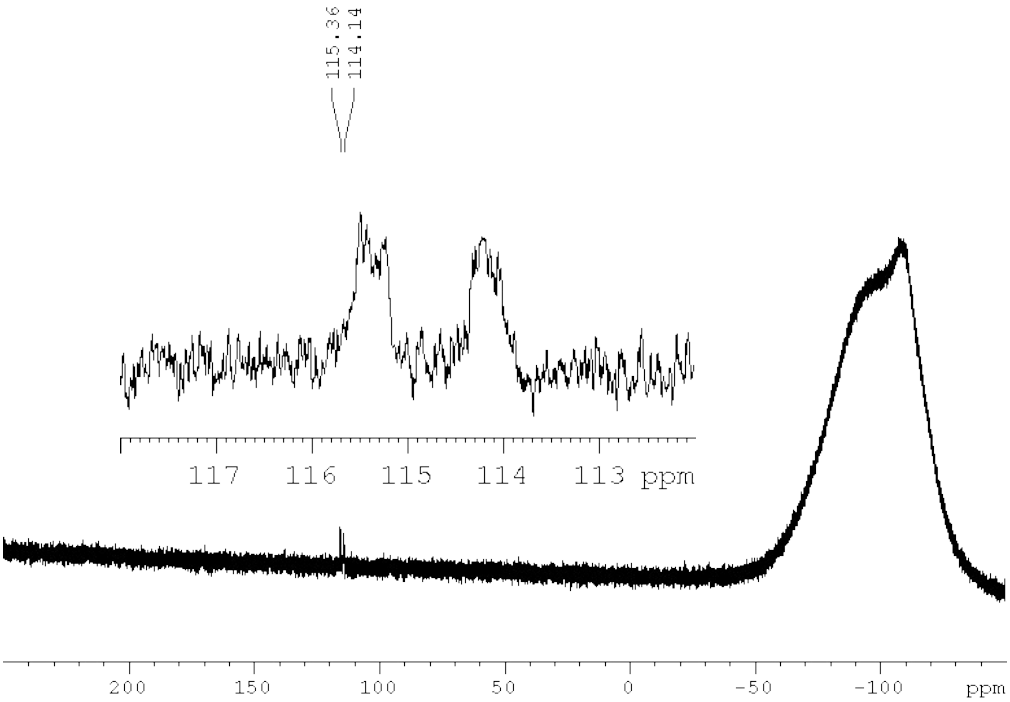

Figure S22. $^{29}Si\{^1H\}$ NMR spectrum of compound [LSi{Fe(CO)$_4$}PH{PtH(PPh$_3$)$_2$}], **6**.

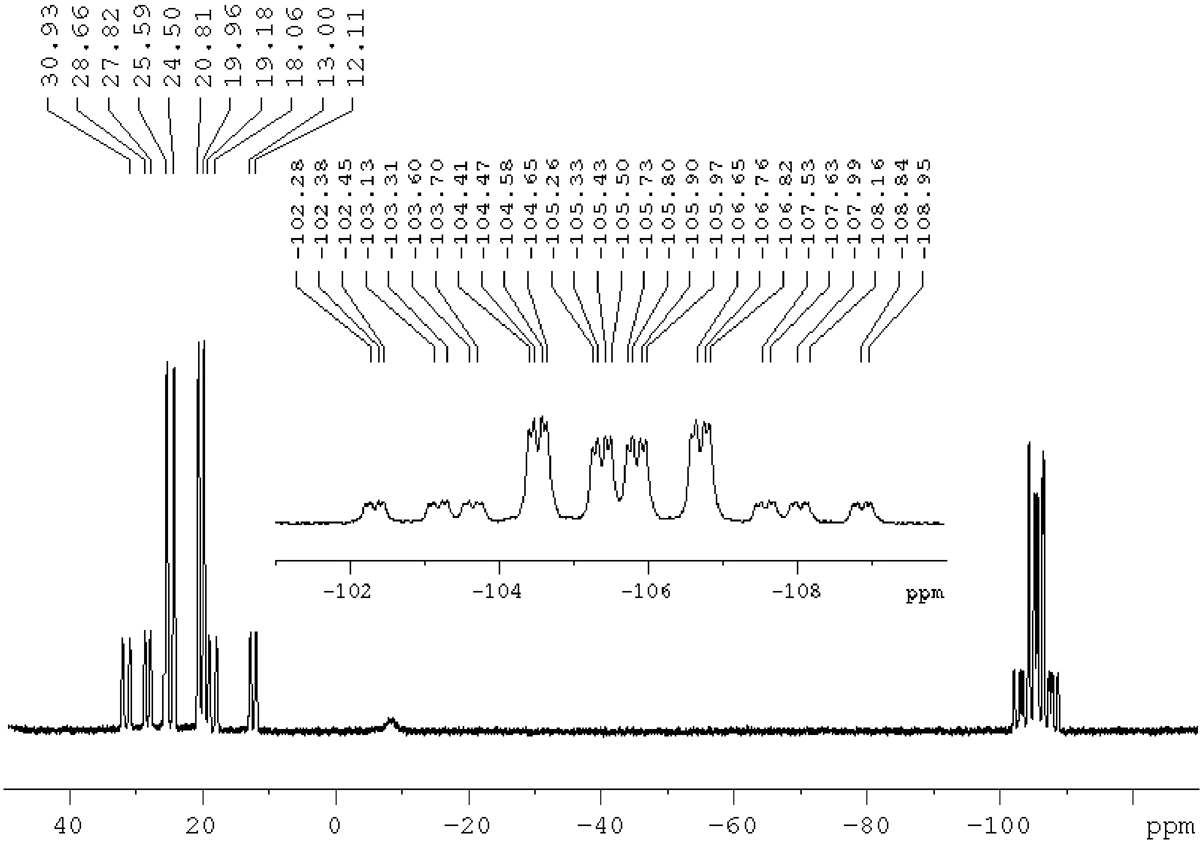

Figure S23. ^{31}P NMR spectrum of compound [LSi{Fe(CO)$_4$}PH{PtH(PPh$_3$)$_2$}], **6**.

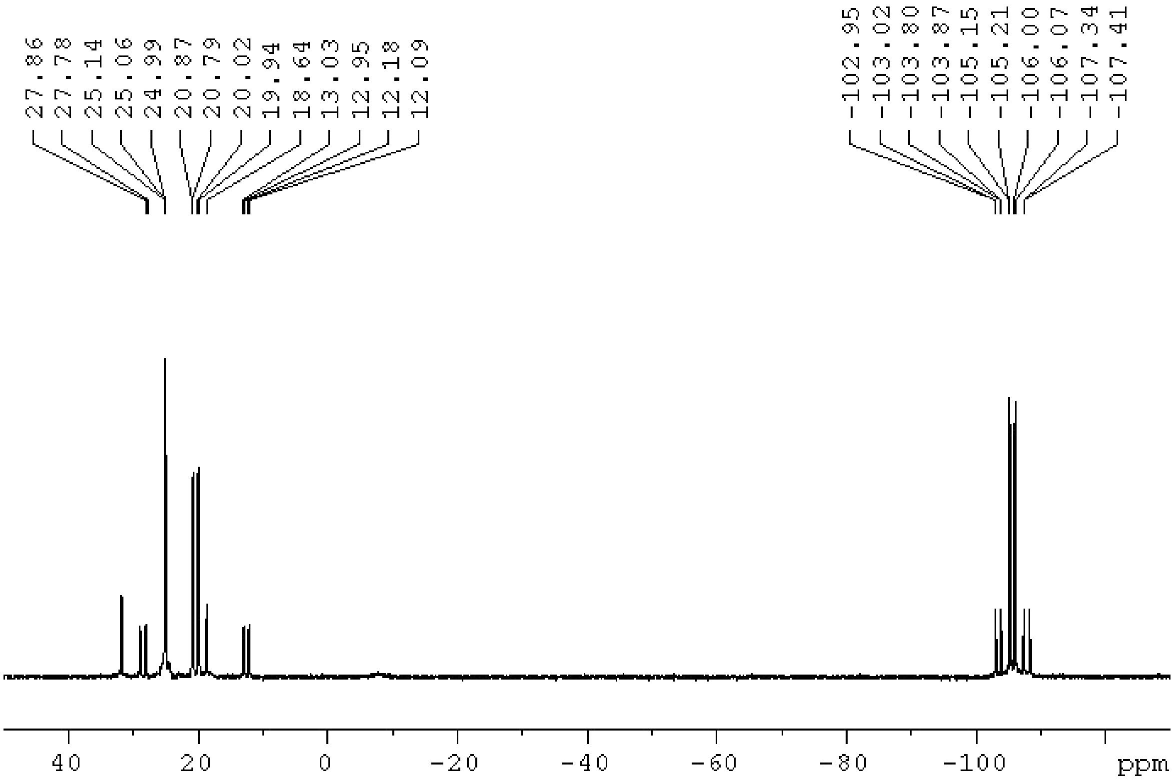

Figure S24. $^{31}P\{^1H\}$ NMR spectrum of compound [LSi{Fe(CO)$_4$}PH{PtH(PPh$_3$)$_2$}], **6**.

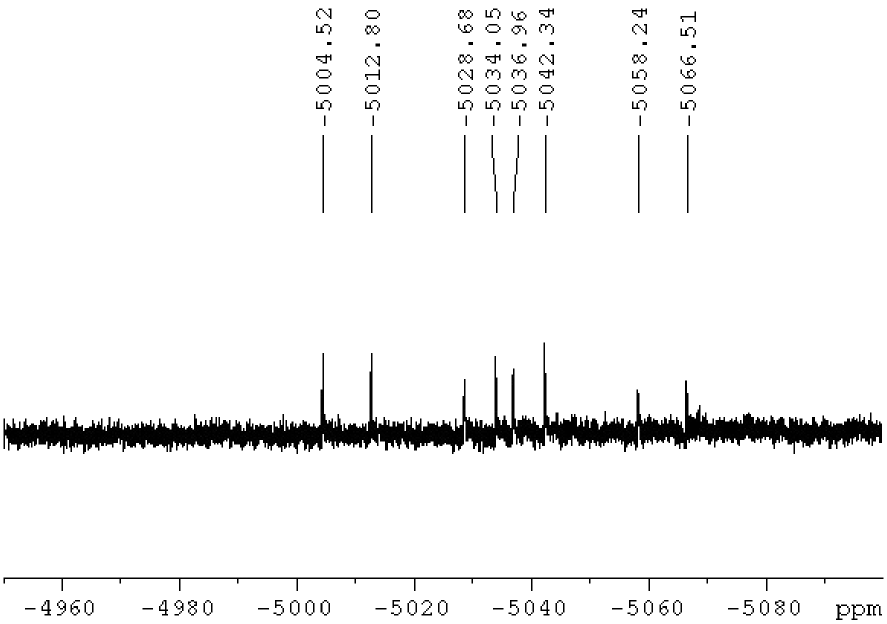

Figure S25. $^{195}Pt\{^1H\}$ NMR spectrum of compound [LSi{Fe(CO)$_4$}PH{PtH(PPh$_3$)$_2$}], **6**.

3. Mass Spectrometry Data of Compounds 2-6.

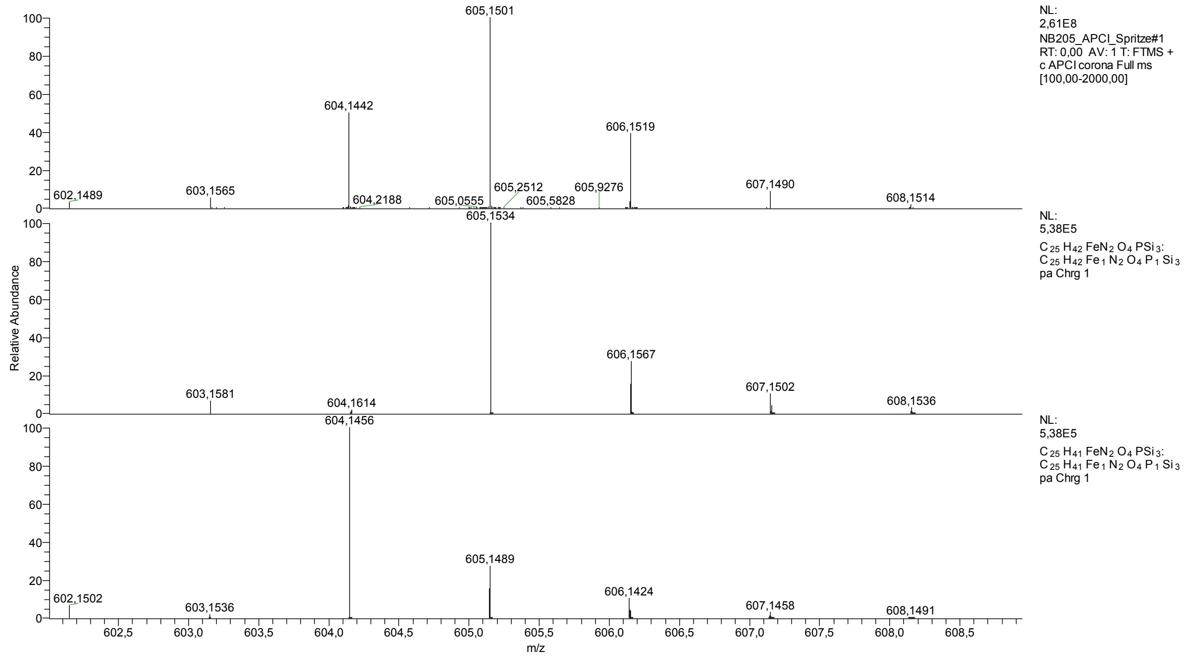

Figure S26. APCI-MS of [MH]⁺ and [M]⁺ signal of **2**. Top (expt.), middle and bottom (theor.).

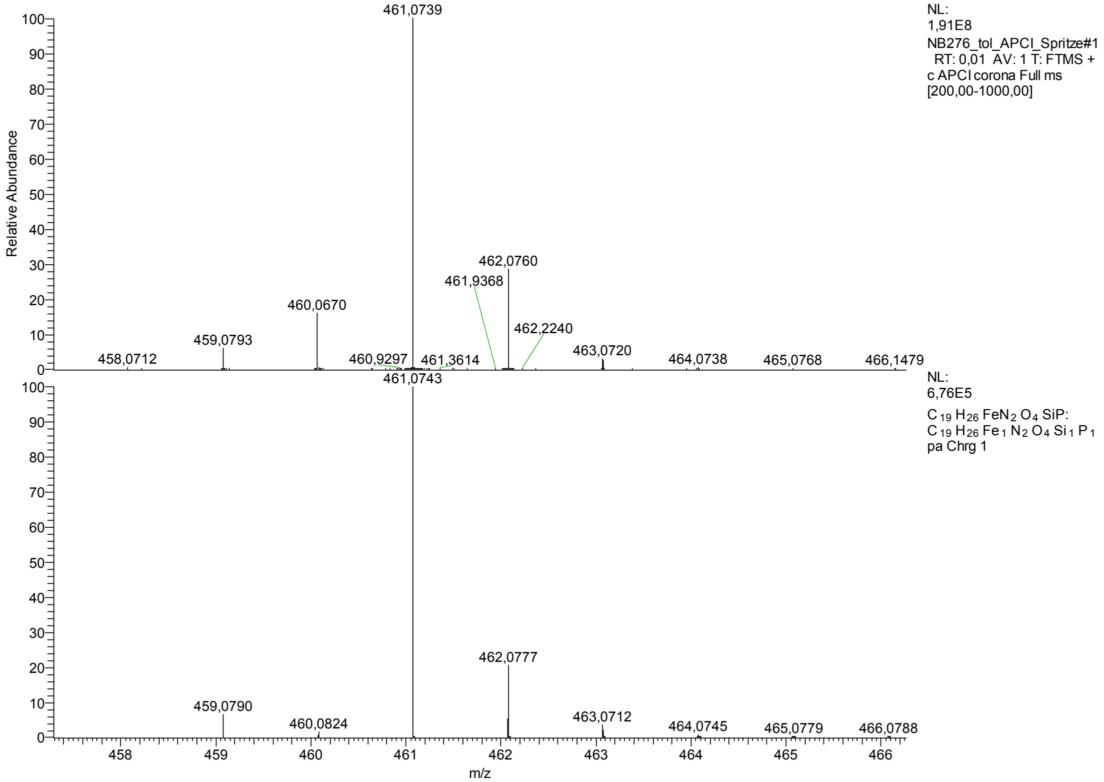

Figure S27. APCI-MS of [M]⁺ signal of **3**. Top (expt.), bottom (theor.).

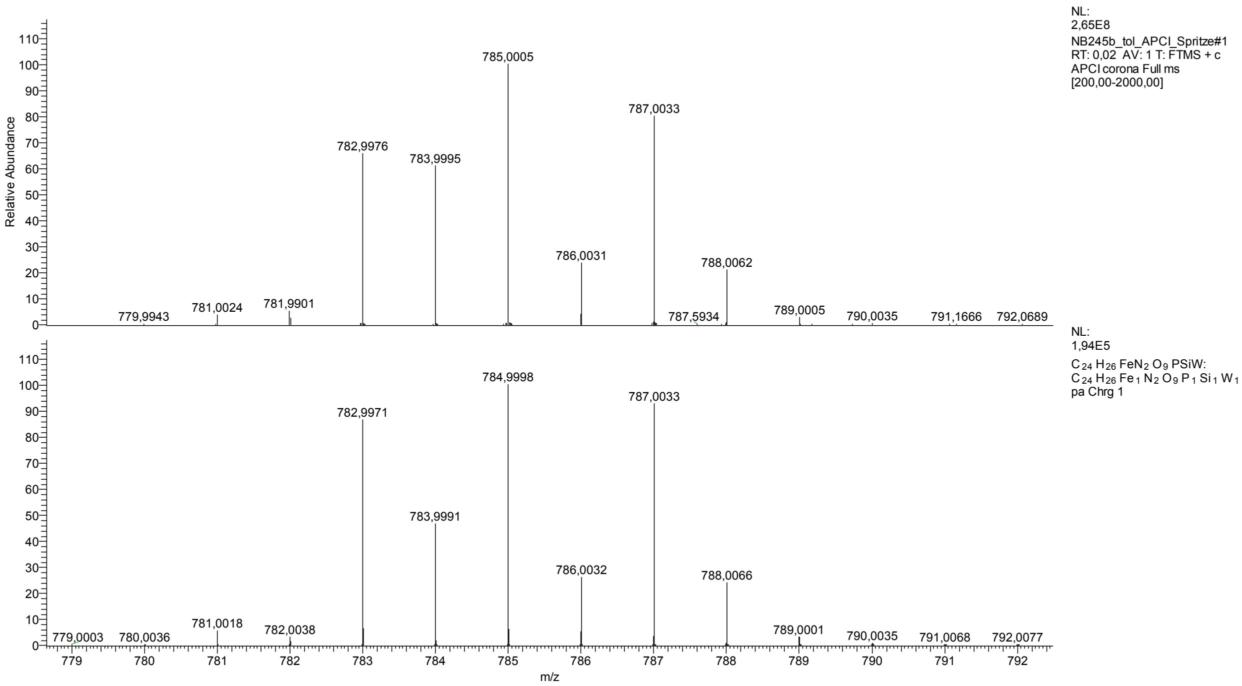

Figure S28. APCI-MS of [MH]$^+$ signal of **4**. Top (expt.), bottom (theor.).

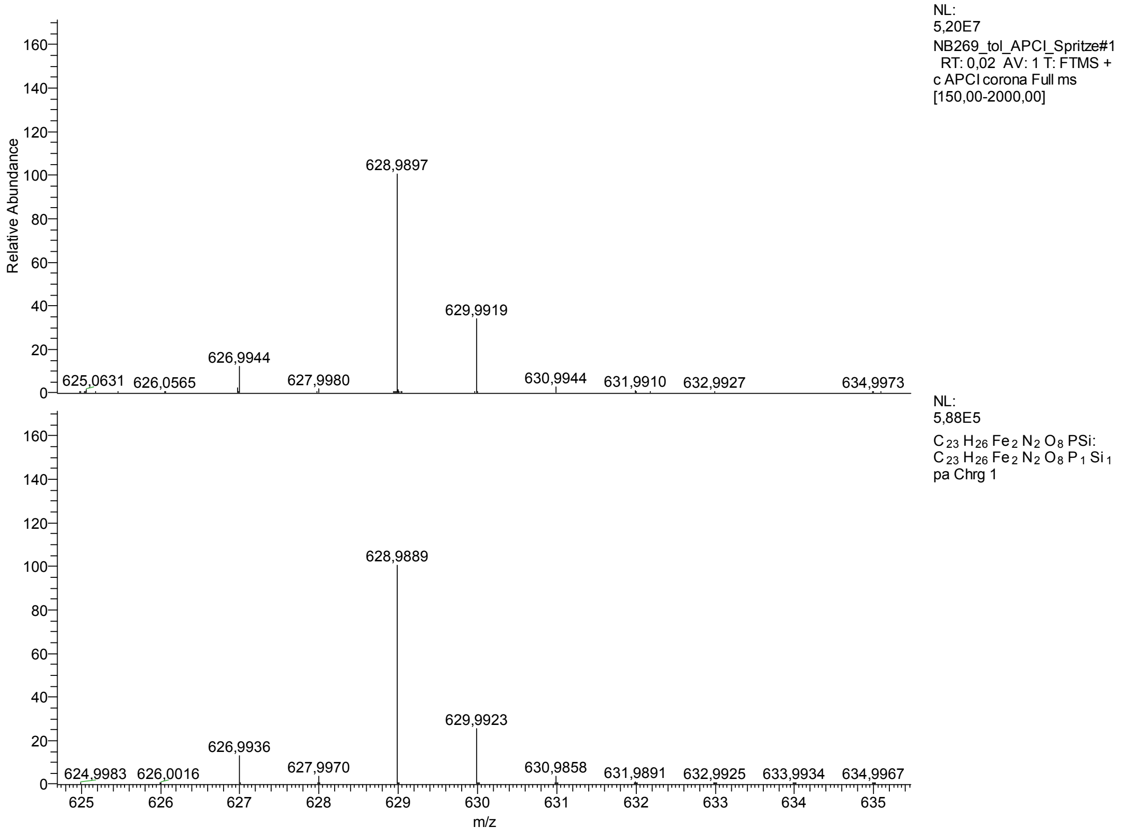

Figure S29. APCI-MS of [MH]$^+$ signal of **5**. Top (expt.), bottom (theor.).

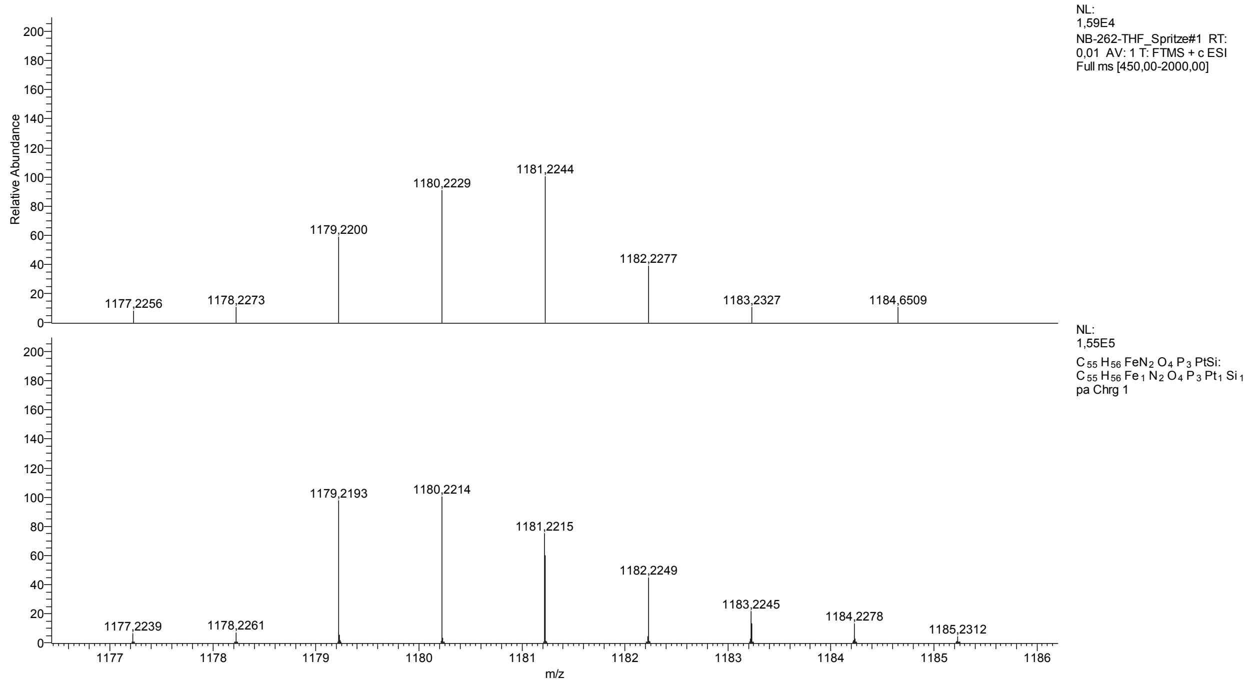

Figure S30. APCI-MS of $[MH]^+$ and $[M]^+$ signal of **6**. Top (expt.), middle and bottom (theor.).

4. IR Data of Compounds 2-6

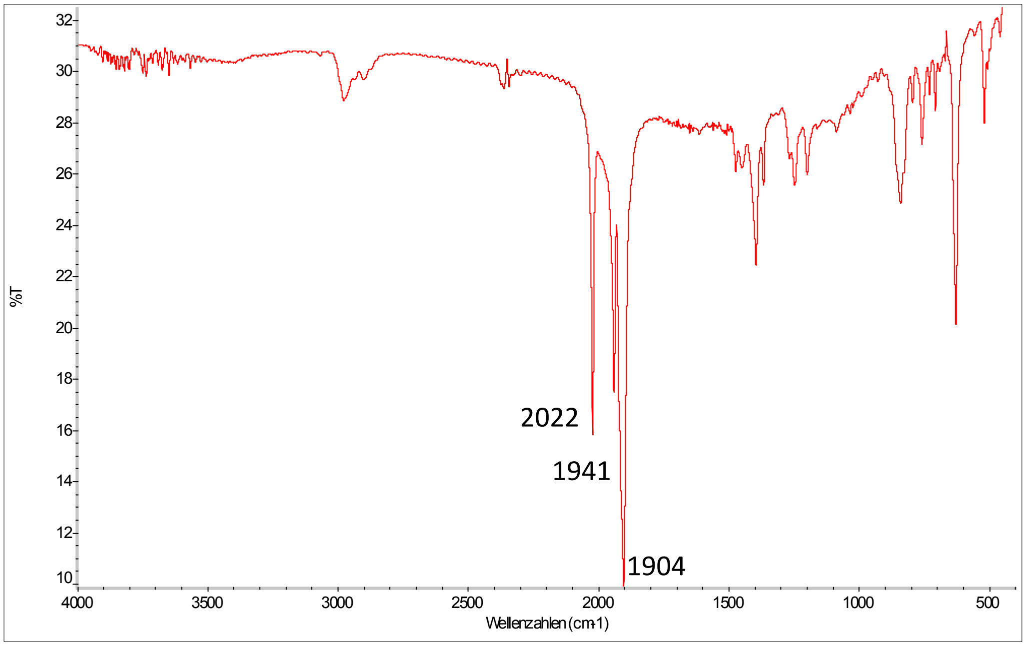

Figure S31. IR spectrum (KBr) of compound **2**.

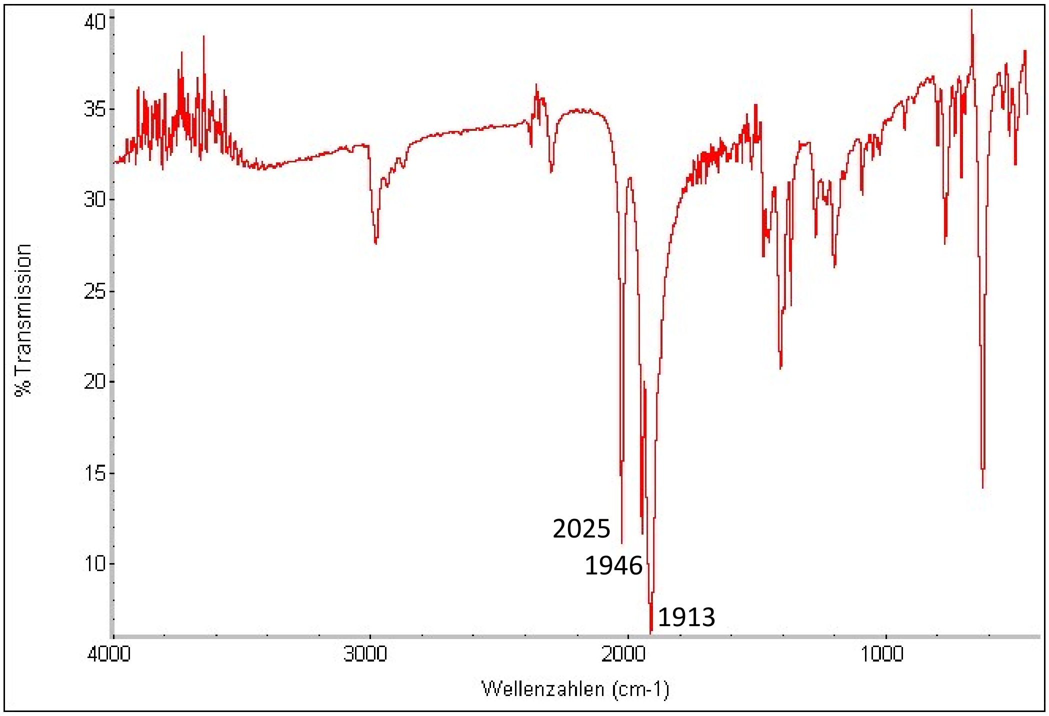

Figure S32. IR spectrum (KBr) of compound **3**.

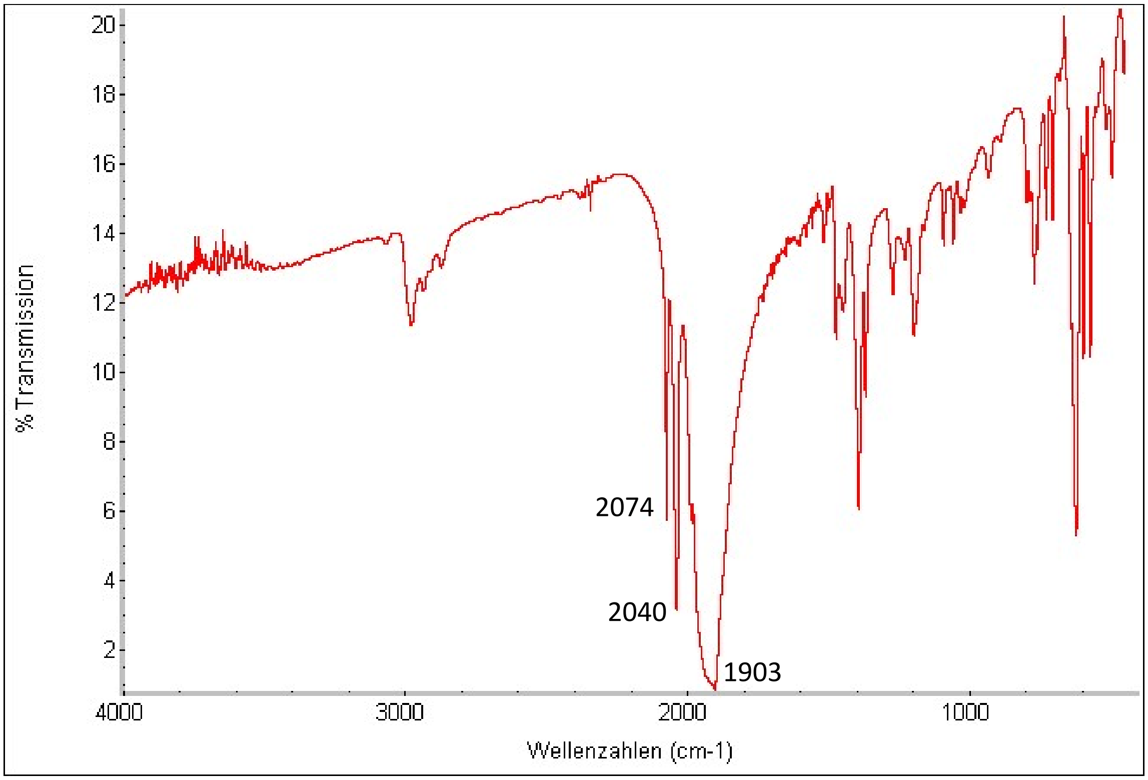

Figure S33. IR spectrum (KBr) of compound **4**.

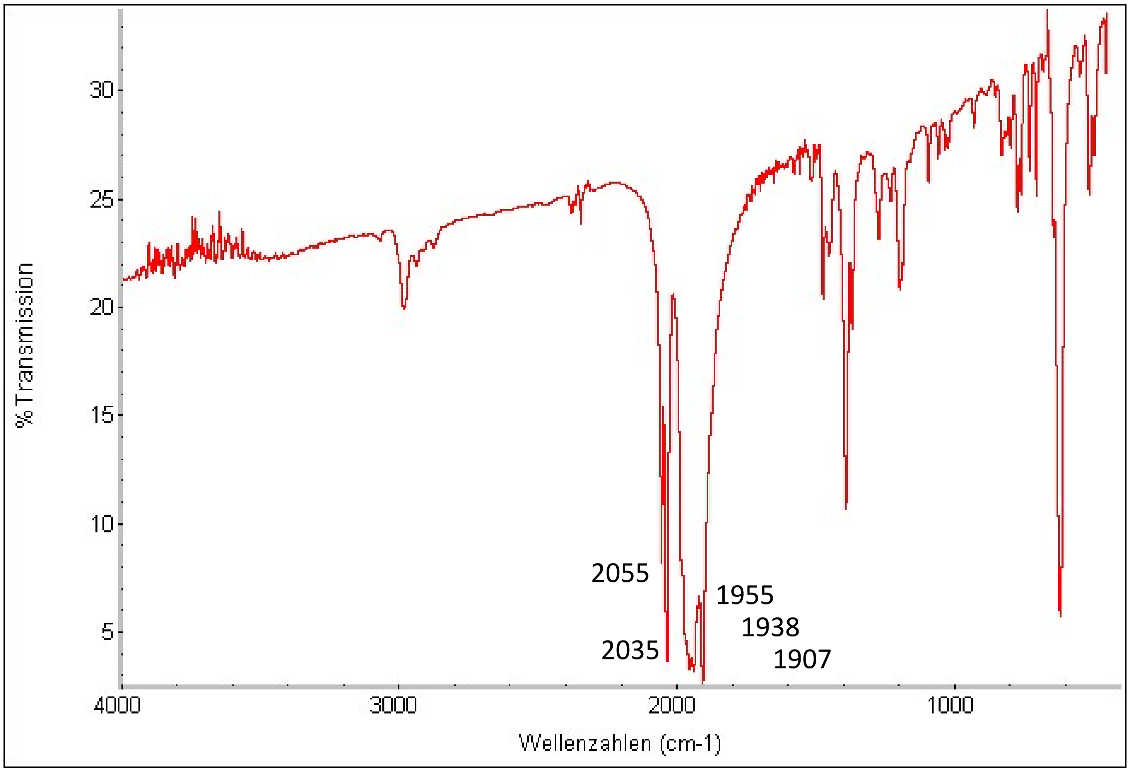

Figure S34. IR spectrum (KBr) of compound **5**.

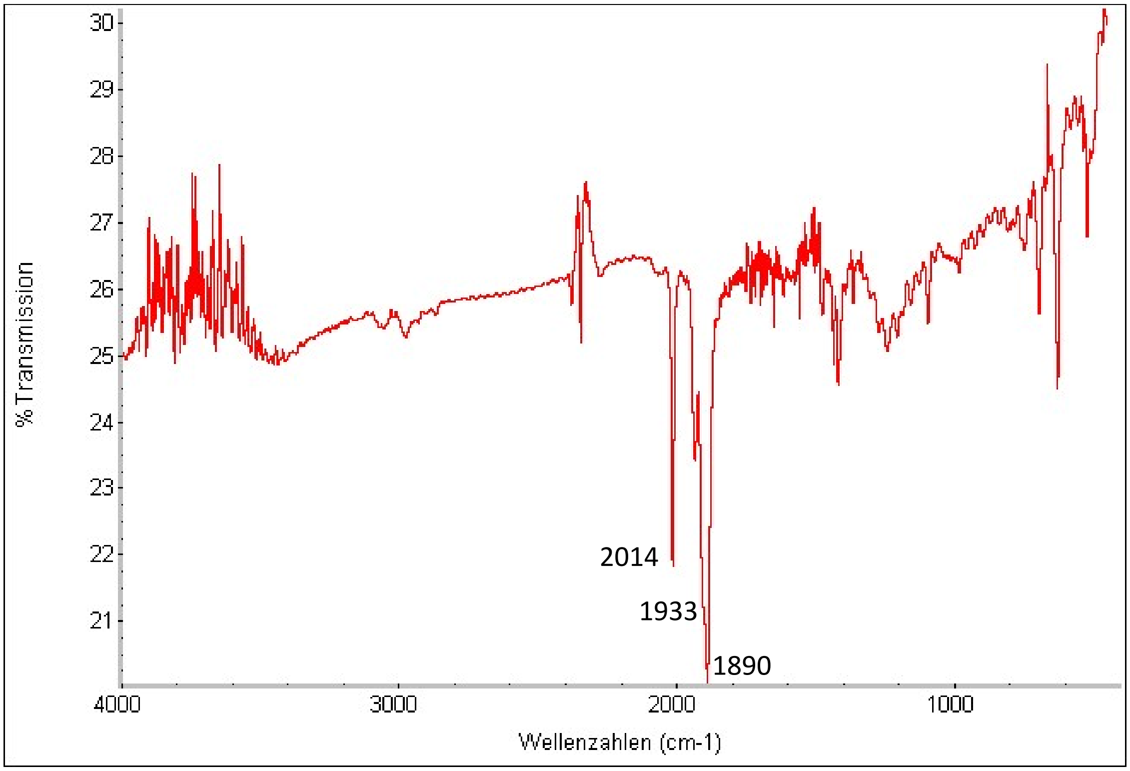

Figure S35. IR spectrum (KBr) of compound **6**.

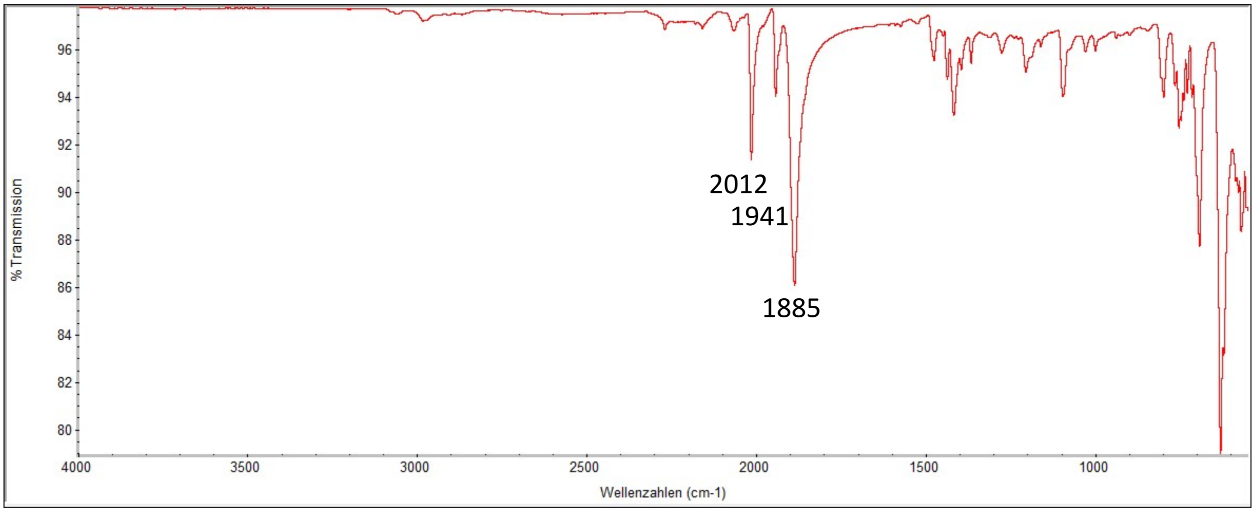

Figure S35. IR spectrum (no matrix) of compound **6**.

5. Cyclic voltammograms of 3 and 6

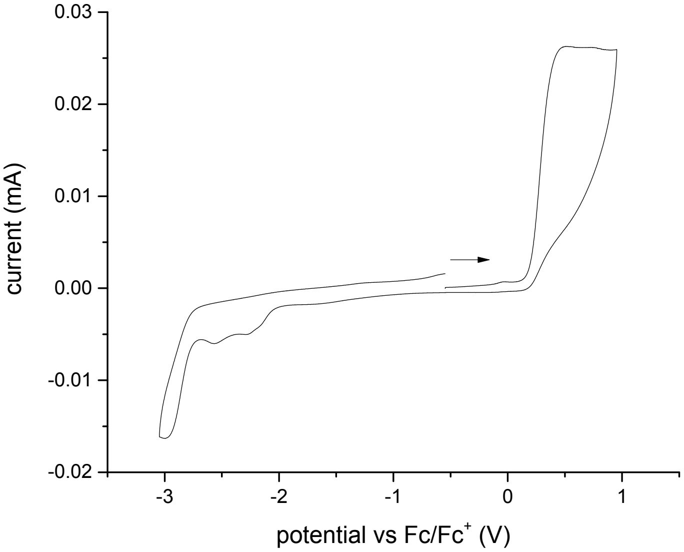

Figure S36. Cyclic voltammogram of **3** (1 mM in thf; 0.1 M [nBu$_4$N][PF$_6$]; scan rate = 100 mV/s) referenced to Cp$_2$Fe/Cp$_2$Fe$^+$ with the oxidation wave being followed by the reduction wave.

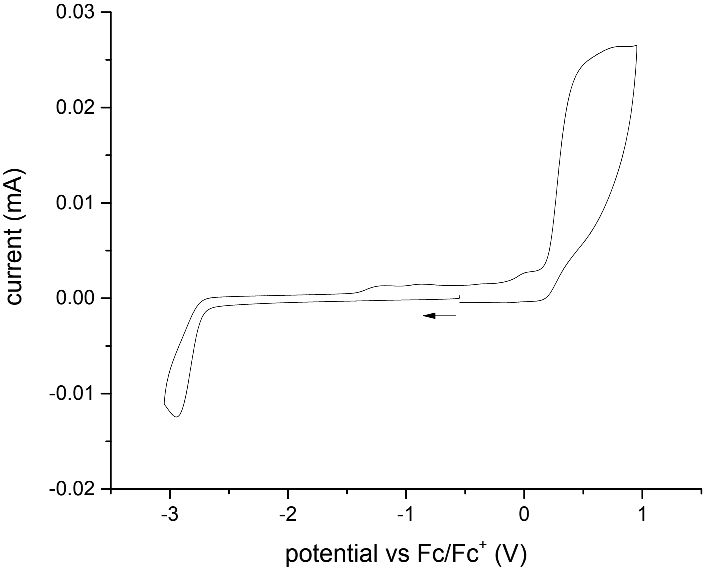

Figure S37. Cyclic voltammogram of **6** (1 mM in thf; 0.1 M [nBu$_4$N][PF$_6$]; scan rate = 100 mV/s) referenced to Cp$_2$Fe/Cp$_2$Fe$^+$ with the reduction wave being followed by the oxidation wave.

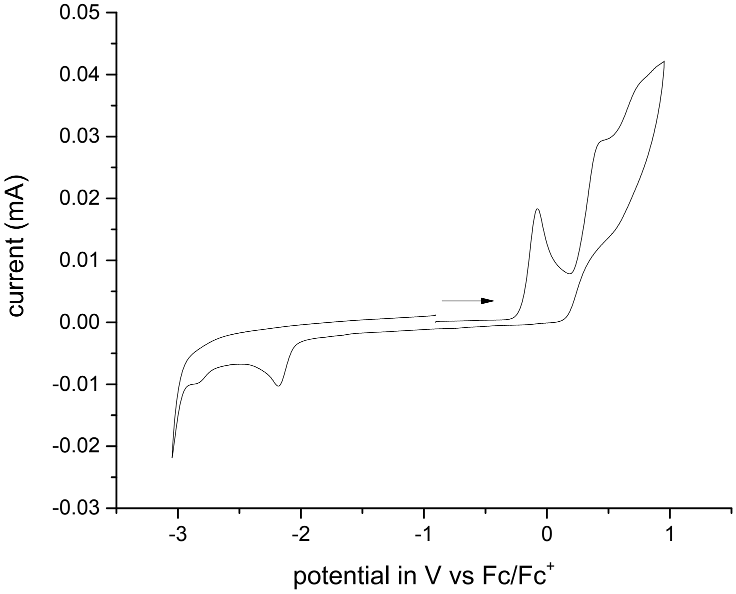

Figure S38. Cyclic voltammogram of **6** (1 mM in thf; 0.1 M [*n*Bu_4N][PF_6]; scan rate = 100 mV/s) referenced to Cp_2Fe/Cp_2Fe^+ with the oxidation wave being followed by the reduction wave.

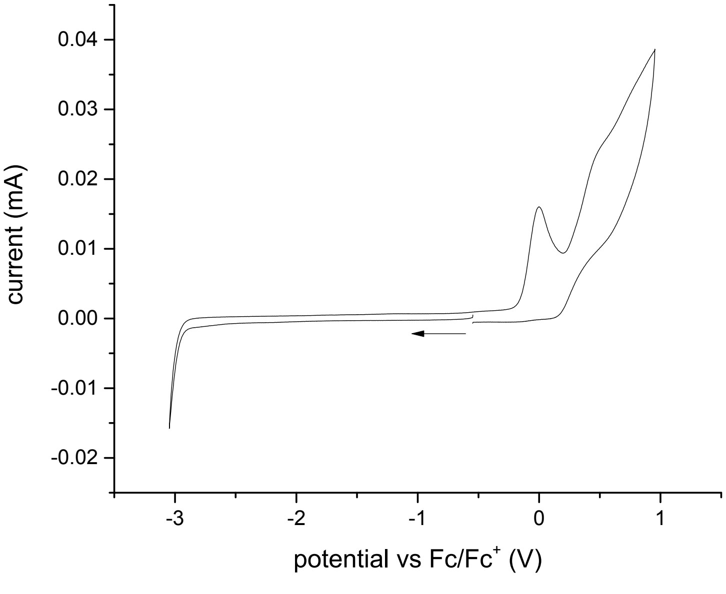

Figure S39. Cyclic voltammogram of **6** (1 mM in thf; 0.1 M [*n*Bu_4N][PF_6]; scan rate = 100 mV/s) referenced to Cp_2Fe/Cp_2Fe^+ with the reduction wave being followed by the oxidation wave.

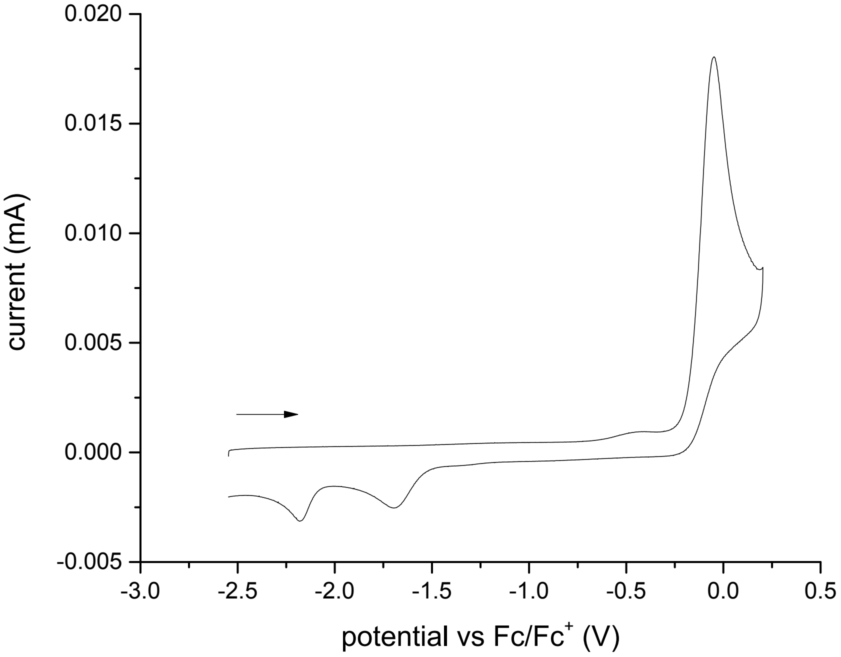

Figure S40. Cyclic voltammogram of **6** (1 mM in thf; 0.1 M [*n*Bu$_4$N][PF$_6$]; scan rate = 100 mV/s) referenced to Cp$_2$Fe/Cp$_2$Fe$^+$ with the oxidation stopping after the first oxidation and subsequent reduction.

Description of the cyclic voltammograms.

The electrochemical behavior of **3** and **6** was studied by cyclic voltammetry to further elucidate the influence of a different transition metal to the electronic properties. Compound **3** exhibits an irreversible oxidation at 0.47 V. No reduction was observed up to -2.5 V without prior oxidation (Figure 37). However, subsequent to oxidation, a reduction event at -2.27 V took place that must be based on the follow up products from the oxidation of **3** (Figure S36). In the cyclic voltammograms of **6**, a similar oxidation wave with a reduction wave only after the oxidation were observed at 0.44 V and -2.18 V (Figure S38 and Figure S39). In addition to those, an irreversible oxidation at -0.08 V was observed. When the oxidation of **6** was stopped after the first oxidation event, this oxidation remained irreversible, but a new reduction event was observed at -1.70 V (Figure S40). While a complete understanding of the oxidation products and their fate would be interesting also considering that to the best of our knowledge nothing is known about the redox chemistry of silylene complexes, it is beyond the scope of this publication. However, the following conclusions can be drawn from the cyclic voltammetry data: The irreversible oxidation at 0.47 V is barely influenced by the presence of platinum, but one additional irreversible oxidation is observed.

6. Single Crystal X-ray Diffraction Data

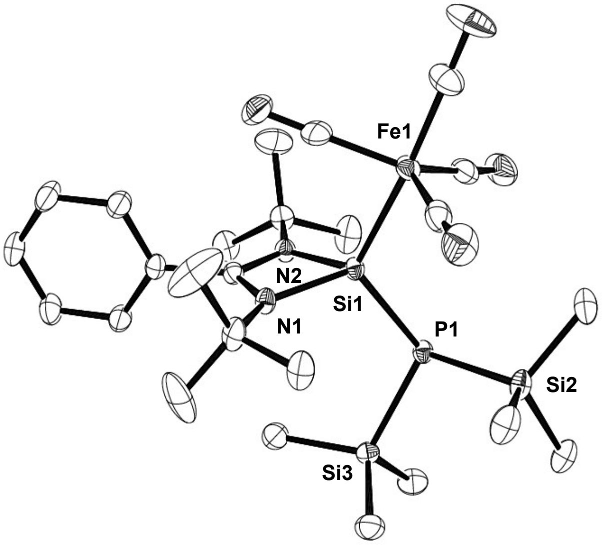

Figure S36. Molecular structure of compound **2**. Thermal ellipsoids are drawn at the 40% probability level. Hydrogen atoms and one disordered *t*Bu group are omitted for clarity. Selected bond lengths (Å) and angles (°) in **2**: P1–Si1 2.2281(6), Fe1–Si1 2.2777(5), P1–Si2 2.2556(6), P1–Si3 2.2598(6), Si1–N1 1.8422(14), Si1–N2 1.8510(14); C22–Fe1–Si1 172.33(9), P1–Si1–Fe1 119.19(2).

Table S1. Crystallographic data and structure refinement for compound **2**.

Empirical formula	$C_{25}H_{41}FeN_2O_4PSi_3$
Formula weight	604.69
Temperature	150(2) K
Wavelength	1.541840 Å
Crystal system	Monoclinic
Space group	P21/n
a/Å	11.16410(10)
b/Å	16.63080(10)
c/Å	17.55870(10)
α/°	90.000(5)
β/°	94.7870(10)
γ/°	90.000(5)
Volume	3248.72(4) Å^3
Z	4
Density (calculated)	1.236 Mg/m^3
Absorption coefficient	5.495 mm^{-1}
F(000)	1280

Crystal size [mm^3]	0.22 x 0.07 x 0.26
Theta range for data collection	3.66 to 73.45º
Index range	–13≤h≤13, –19≤k≤19, –19≤l≤21
Reflections collected	5845
Independent reflections	5375
Absorption correction	Semi-empirical from equivalents
Refinement method	Full-matrix least-squares on F^2
Data / restraints / parameters	5845 / 0 / 368
Goodness-of-fit on F^2	1.029
Final R indices [I>2sigma(I)]	R1 = 0.0304, wR2 = 0.0789
R indices (all data)	R1 = 0.0338, wR2 = 0.0810

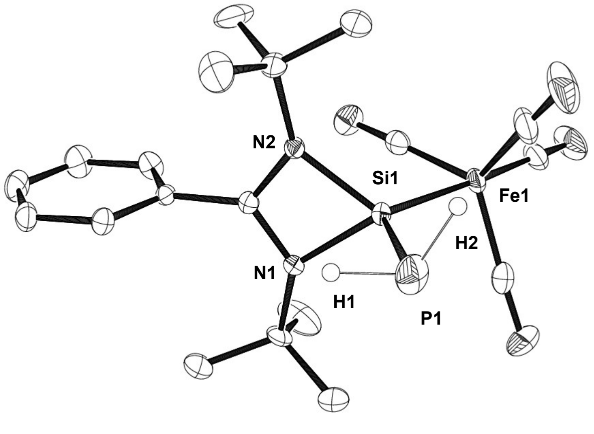

Figure S37. Molecular structure of compound **3**. Thermal ellipsoids are drawn at 40% probability level. Hydrogen atoms except for H1 and H2 are omitted for clarity. Selected bond length (Å) and angles (°) in **3**: Si1 P1 2.2551(9), Fe1 Si1 2.2412(7), Si1 N1 1.8355(19), Si1 N2 1.8291(19), Fe1 Si1 P1 119.97(3), N1 Si1 P1 105.20(7), N2 Si1 P1 107.35(7), N1 Si1 Fe1 121.93(7), N2 Si1 Fe1 120.75(6).

Table S2. Crystallographic data and structure refinement for compound **3**.

Empirical formula	$C_{19}H_{25}FeN_2O_4PSi$
Formula weight	460.32
Temperature	150(2) K
Wavelength	1.541840 Å
Crystal system	Orthorhombic
Space group	P212121
a/Å	12.57230(10)
b/Å	13.31840(10)
c/Å	13.69390(10)
α/°	90.00
β/°	90.00
γ/°	90.00
Volume	2292.95(3) Å^3
Z	4
Density (calculated)	1.333 Mg/m^3
Absorption coefficient	6.653 mm^{-1}
F(000)	960
Crystal size [mm^3]	0.35 x 0.22 x 0.16
Theta range for data collection	3.23 to 73.45º
Index range	$-8 \le h \le 15$, $-15 \le k \le 15$, $-15 \le l \le 16$
Reflections collected	4089
Independent reflections	3861
Absorption correction	Semi-empirical from equivalents
Refinement method	Full-matrix least-squares on F^2
Data / restraints / parameters	4089 / 0 / 267
Goodness-of-fit on F^2	1.041
Final R indices [I>2sigma(I)]	R1 = 0.0301, wR2 = 0.0756
R indices (all data)	R1 = 0.0333, wR2 = 0.0774

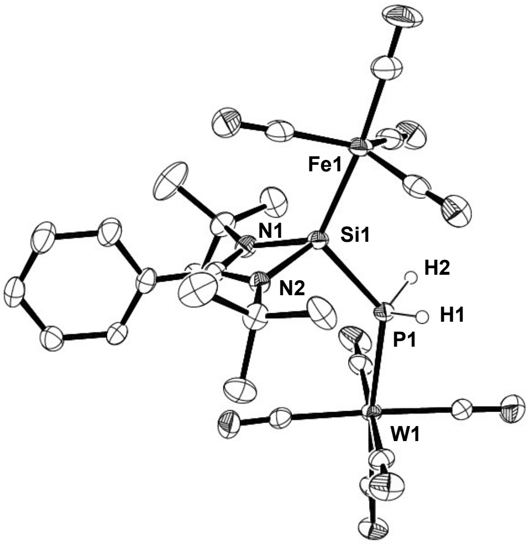

Figure S38. Molecular structure of compound **4**. Thermal ellipsoids are drawn at 40% probability level. Hydrogen atoms except for H1 and H2, the disorder of the *t*Bu group and one molecule of pentane are omitted for clarity. Selected bond length (Å) and angles (°) in **4**. Si1 P1 2.2790(13), Si1 Fe1 2.2307(10), P1 W1 2.5194(8), Si1 N1 1.823(3), Si1 N2 1.821(3), P1 Si1 Fe1 116.45(5), Si1 P1 W1 135.28(5), N1 Si1 N2 71.95(12), P1 W1 C20 173.35(10), Si1 Fe1 C16 172.55(15).

Table S3. Crystallographic data and structure refinement for compound **4**.

Empirical formula	$C_{53}H_{62}Fe_2N_4O_{18}P_2Si_2W_2$
Formula weight	1640.59
Temperature	150(2) K
Wavelength	1.541840 Å
Crystal system	Monoclinic
Space group	C2/c
a/Å	25.6547(2)
b/Å	10.40180(10)
c/Å	24.8836(2)
α/°	90.00
β/°	91.7970(10)
γ/°	90.00
Volume	6637.05(10) Å^3
Z	4
Density (calculated)	1.642 Mg/m^3
Absorption coefficient	11.045 mm^{-1}
F(000)	3240
Crystal size [mm^3]	0.40 x 0.13 x 0.09

Theta range for data collection	3.54 to 73.54º
Index range	–20≤h≤30, –12≤k≤12, –29≤l≤29
Reflections collected	5984
Independent reflections	5623
Absorption correction	Semi-empirical from equivalents
Refinement method	Full-matrix least-squares on F^2
Data / restraints / parameters	5984 / 150 / 484
Goodness-of-fit on F^2	1.055
Final R indices [I>2sigma(I)]	R1 = 0.0310, wR2 = 0.0803
R indices (all data)	R1 = 0.0334, wR2 = 0.0827

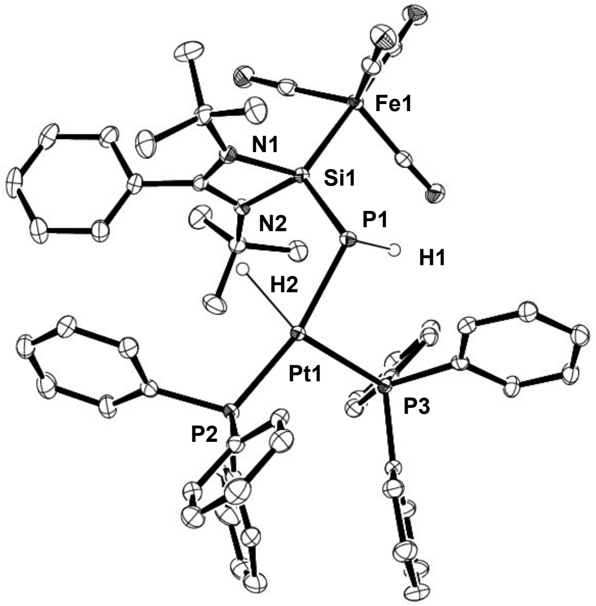

Figure S39. Molecular structure of compound **6**. Thermal ellipsoids are drawn at 40% probability level. Hydrogen atoms except for H1 and H2 and two molecules of thf are omitted for clarity. Selected bond length (Å) and angles (°) in **6**: Si1 P1 2.2176(11), Fe1 Si1 2.2917(9), Pt1 P1 2.3341(7), Pt1 P2 2.2854(8), Pt1 P3 2.3301(7), Si1 N1 1.843(3), Si1 N2 1.846(3), P2 Pt1 P1 164.20(3), P3 Pt1 P1 92.37(3), P2 Pt1 P3 102.05(3), C16 Fe1 Si1 174.95(11), N1 Si1 N2 71.17(12), P1 Si1 Fe1 118.76(4), Si1 P1 Pt1 113.70(4).

Table S4. Crystallographic data and structure refinement for compound **6**.

Empirical formula	$C_{63}H_{71}FeN_2O_6P_3PtSi$
Formula weight	1324.16
Temperature	150(2) K
Wavelength	1.541840 Å
Crystal system	Triclinic
Space group	P-1
a/Å	12.5026(4)
b/Å	14.9669(5)
c/Å	17.0989(6)
α/°	74.135(3)
β/°	76.241(3)
γ/°	88.008(3)
Volume	2987.87(17) Å^3
Z	2
Density (calculated)	1.472 Mg/m^3
Absorption coefficient	7.624 mm^{-1}
F(000)	1348
Crystal size [mm^3]	0.23 x 0.12 x 0.07
Theta range for data collection	2.75 to 73.57º
Index range	–14≤h≤13, –17≤k≤17, –19≤l≤20
Reflections collected	10737
Independent reflections	10198
Absorption correction	Semi-empirical from equivalents
Refinement method	Full-matrix least-squares on F^2
Data / restraints / parameters	10737 / 0 / 708
Goodness-of-fit on F^2	1.034
Final R indices [I>2sigma(I)]	R1 = 0.0321, wR2 = 0.0875
R indices (all data)	R1 = 0.0347, wR2 = 0.0898

5. References

[1] a) N. C. Breit, T. Szilvási and S. Inoue, *Chem. Eur. J.*, 2014, **20**, 9312; b) S. Inoue, W. Wang, C. Präsang, M. Asay, E. Irran, M. Driess, *J. Am. Chem. Soc.* 2011, **133**, 2869.

[2] G. M. Sheldrick, SHELX-97 Program for Crystal Structure Determination, Universitat Göttingen: Göttingen, Germany, 1997.

[3] C. F. Macrae, P. R. Edgington, P. McCabe, E. Pidcock, G. P. Shields, R. Taylor, M. Towler and J. van de Streek, *J. Appl. Cryst.*, 2006, **39**, 453.